the case of the untreated patients might due to a multiplicity of CML subclones.

CML patients develop imatinib resistance through either Bcr-Abl dependent or independent mechanisms. The most characterized and frequent mechanism is the acquisition of point mutations within the kinase domain of the Bcr-Abl gene, and some of the mutations such as T315I are potent predictors for outcome. However, even in those patients who have some mutations other than a few restricted mutations such as T315I and F317L, we cannot accurately predict the efficacy of TKIs. Furthermore, nearly half of the patients resistant to imatinib have no mutations in Bcr-Abl, which indicates that other mechanisms are also important for the acquisition of drug-resistance. Thus, we need other information for selecting TKIs. In this study, 4 patients carried point mutations in this region. Samples from 3 of them had RI values compatible with the predictive outcomes from the mutations. Notably, the RI values of the other sample contradicted the response of the mutation, but accorded with the actual response of the patient. From these points of view, the system described here can be utilized as another powerful predictor than IC50s for Bcr-Abl mutations.

The immunoblot system described here has the capacity to detect TKI-resistant subclones, including CML cells with Bcr-Abl mutations. In addition, our strategy seems to evaluate Bcr-Abl activity more directly than the cellular IC50 and require smaller population of TKI-resistant subclones than Bcr-Abl sequence analysis. Thus, when used together with the cellular IC50 values and Bcr-Abl sequence, this immunoblot system should help improve the treatment of patients with CML.

Conflict of interest

The authors state that they have no conflict of interest.

Acknowledgements

We would like to thank Shibano M. (Sakai Munincipal Hospital, Sakai, Japan), Sugahara H. (Sumitomo Hospital, Osaka, Japan), Moriyama Y. (Ikeda City Hospital, Ikeda, Japan), Azenishi Y. (Minoh City Hospital, Minoh, Japan), Ishida N. (Itami City Hospital, Itami, Japan), and Yamada M. (Suita Munincipal Hospital, Suita, Japan), who kindly provided blood samples.

References

[1] Kantarjian H, Sawyers C, Hochhaus A, Guilhot F, Schiffer C, Gambacorti-Passerini C, et al. Hematologic and cytogenetic responses to imatinib mesylate in chronic myelogenous leukemia. N Engl J Med 2002;346:645–52.
[2] O'Brien SG, Guilhot F, Larson RA, Gathmann I, Baccarani M, Cervantes F, et al. Imatinib compared with interferon and low-dose cytarabine for newly diagnosed chronic-phase chronic myeloid leukemia. N Engl J Med 2003;348:994–1004.
[3] Sawyers CL, Hochhaus A, Feldman E, Goldman JM, Miller CB, Ottmann OG, et al. Imatinib induces hematologic and cytogenetic responses in patients with chronic myelogenous leukemia in myeloid blast crisis: results of a phase II study. Blood 2002;99:3530–9.
[4] Talpaz M, Silver RT, Druker BJ, Goldman JM, Gambacorti-Passerini C, Guilhot F, et al. Imatinib induces durable hematologic and cytogenetic responses in patients with accelerated phase chronic myeloid leukemia: results of a phase 2 study. Blood 2002;99:1928–37.
[5] Druker BJ, Sawyers CL, Kantarjian H, Resta DJ, Reese SF, Ford JM, et al. Activity of a specific inhibitor of the BCR-ABL tyrosine kinase in the blast crisis of chronic myeloid leukemia and acute lymphoblastic leukemia with the Philadelphia chromosome. N Engl J Med 2001;344:1038–42.
[6] Azam M, Latek RR, Daley GQ. Mechanisms of autoinhibition and STI-571/imatinib resistance revealed by mutagenesis of BCR-ABL. Cell 2003;112:831–43.
[7] Donato NJ, Wu JY, Stapley J, Gallick G, Lin H, Arlinghaus R, et al. BCR-ABL independence and LYN kinase overexpression in chronic myelogenous leukemia cells selected for resistance to STI571. Blood 2003;101:690–8.
[8] Weisberg E, Manley PW, Breitenstein W, Bruggen J, Cowan-Jacob SW, Ray A, et al. Characterization of AMN107, a selective inhibitor of native and mutant Bcr-Abl. Cancer Cell 2005;7:129–41.
[9] Talpaz M, Shah NP, Kantarjian H, Donato N, Nicoll J, Paquette R, et al. Dasatinib in imatinib-resistant Philadelphia chromosome-positive leukemias. N Engl J Med 2006;354:2531–41.
[10] Boschelli DH, Wu B, Ye F, Wang Y, Golas JM, Lucas J, et al. Synthesis and Src kinase inhibitory activity of a series of 4-[(2,4-dichloro-5-methoxyphenyl)amino]-7-furyl-3-quinolinecarbonitriles. J Med Chem 2006;49:7868–76.
[11] Kimura S, Naito H, Segawa H, Kuroda J, Yuasa T, Sato K, et al. NS-187, a potent and selective dual Bcr-Abl/Lyn tyrosine kinase inhibitor, is a novel agent for imatinib-resistant leukemia. Blood 2005;106:3948–54.
[12] Saglio G, Kim DW, Issaragrisil S, le Coutre P, Etienne G, Lobo C, et al. Nilotinib versus imatinib for newly diagnosed chronic myeloid leukemia. N Engl J Med 2010;362:2251–9.
[13] Kantarjian H, Shah NP, Hochhaus A, Cortes J, Shah S, Ayala M, et al. Dasatinib versus imatinib in newly diagnosed chronic-phase chronic myeloid leukemia. N Engl J Med 2010;362:2260–70.
[14] Wei G, Rafiyath S, Liu D. First-line treatment for chronic myeloid leukemia: dasatinib, nilotinib, or imatinib. J Hematol Oncol 2010;3:47–56.
[15] Baccarani M, Saglio G, Goldman J, Hochhaus A, Simonsson B, Appelbaum F, et al. Evolving concepts in the management of chronic myeloid leukemia: recommendations from an expert panel on behalf of the European LeukemiaNet. Blood 2006;108:1809–20.
[16] Baccarani M, Rosti G, Castagnetti F, Haznedaroglu I, Porkka K, Abruzzese E, et al. Comparison of imatinib 400 mg and 800 mg daily in the front-line treatment of high-risk, Philadelphia-positive chronic myeloid leukemia: a European LeukemiaNet Study. Blood 2009;113:4497–504.
[17] Tokunaga M, Ezoe S, Tanaka H, Satoh Y, Fukushima K, Matsui K, et al. BCR-ABL but not JAK2 V617F inhibits erythropoiesis through the Ras signal by inducing p21CIP1/WAF1. J Biol Chem 2010;285:31774–82.
[18] Ezoe S, Matsumura I, Nakata S, Gale K, Ishihara K, Minegishi N, et al. GATA-2/estrogen receptor chimera regulates cytokine-dependent growth of hematopoietic cells through accumulation of p21(WAF1) and p27(Kip1) proteins. Blood 2002;100:3512–20.
[19] Tanaka C, Yin OQ, Sethuraman V, Smith T, Wang X, Grouss K, et al. Clinical pharmacokinetics of the BCR-ABL tyrosine kinase inhibitor nilotinib. Clin Pharmacol Ther 2010;87:197–203.
[20] Peng B, Hayes M, Resta D, Racine-Poon A, Druker BJ, Talpaz M, et al. Pharmacokinetics and pharmacodynamics of imatinib in a phase I trial with chronic myeloid leukemia patients. J Clin Oncol 2004;22:935–42.
[21] Luo FR, Yang Z, Camuso A, Smykla R, McGlinchey K, Fager K, et al. Dasatinib (BMS-354825) pharmacokinetics and pharmacodynamic biomarkers in animal models predict optimal clinical exposure. Clin Cancer Res 2006;12:7180–6.
[22] White D, Saunders V, Lyons AB, Branford S, Grigg A, To LB, et al. In vitro sensitivity to imatinib-induced inhibition of ABL kinase activity is predictive of molecular response in patients with de novo CML. Blood 2005;106:2520–6.
[23] von Bubnoff N, Schneller F, Peschel C, Duyster J. BCR-ABL gene mutations in relation to clinical resistance of Philadelphia-chromosome-positive leukaemia to STI571: a prospective study. Lancet 2002;359:487–91.
[24] von Bubnoff N, Veach DR, Miller WT, Li W, Sanger J, Peschel C, et al. Inhibition of wild-type and mutant Bcr-Abl by pyrido-pyrimidine-type small molecule kinase inhibitors. Cancer Res 2003;63:6395–404.
[25] von Bubnoff N, Veach DR, van der Kuip H, Aulitzky WE, Sanger J, Seipel P, et al. A cell-based screen for resistance of Bcr-Abl-positive leukemia identifies the mutation pattern for PD166326, an alternative Abl kinase inhibitor. Blood 2005;105:1652–9.
[26] O'Hare T, Walters DK, Stoffregen EP, Sherbenou DW, Heinrich MC, Deininger MW, et al. Combined Abl inhibitor therapy for minimizing drug resistance in chronic myeloid leukemia: Src/Abl inhibitors are compatible with imatinib. Clin Cancer Res 2005;11:6987–93.

Please cite this article in press as: Shibata M, et al. Predictability of the response to tyrosine kinase inhibitors via *in vitro* analysis of Bcr-Abl phosphorylation. Leuk Res (2011), doi:10.1016/j.leukres.2011.01.012

Immunology Letters 136 (2011) 61–73

Contents lists available at ScienceDirect

Immunology Letters

journal homepage: www.elsevier.com/locate/immlet

Myeloid neoplasm-related gene abnormalities differentially affect dendritic cell differentiation from murine hematopoietic stem/progenitor cells

Jiro Fujita, Masao Mizuki*, Masayasu Otsuka, Sachiko Ezoe, Hirokazu Tanaka, Yusuke Satoh, Kentaro Fukushima, Masahiro Tokunaga, Itaru Matsumura, Yuzuru Kanakura

Department of Hematology and Oncology, Osaka University Graduate School of Medicine, 2-2, Yamadaoka, Suita, Osaka 565-0871, Japan

ARTICLE INFO

Article history:
Received 7 June 2010
Received in revised form 6 December 2010
Accepted 22 December 2010
Available online 13 January 2011

Keywords:
DC culture
Leukemia
Myelodysplastic syndrome
Tyrosine kinase
Transcription factor
Tumor immunology

ABSTRACT

Dendritic cells (DCs) play important roles in tumor immunology. Leukemic cells in patients with myeloid neoplasms can differentiate into DCs *in vivo* (referred to as *in vivo* leukemic DCs), which are postulated to affect anti-leukemia immune responses. We established a reproducible culture system of *in vitro* FLT3 ligand-mediated DC (FL-DC) differentiation from murine lineage$^-$ Sca-1$^+$ c-Kit^{high} cells (LSKs), which made it possible to analyse the effects of target genes on steady-state DC differentiation from hematopoietic stem/progenitor cells. Using this system, we analysed the effects of various myeloid neoplasm-related gene abnormalities, termed class I and class II mutations, on FL-DC differentiation from LSKs. All class II mutations uniformly impaired FL-DC differentiation maintaining a plasmacytoid DC (pDC)/conventional DC (cDC) ratio comparable to the control cells. In contrast, class I mutations differentially affected FL-DC differentiation from LSKs. FLT3-ITD and a constitutively active form of Ras (CA-N-Ras) yielded more FL-DCs than the control, whereas the other class I mutations tested yielded less FL-DCs. Both FLT3-ITD and FLT3-tyrosine kinase domain (TKD) mutation showed a comparable pDC/cDC ratio as the control. CA-N-Ras, c-Kit-TKD, TEL/PDGFRβ, and FIP1L1/PDGFRα showed a severe decrease in the pDC/cDC ratio. CA-STAT5 and CA-MEK1 severely inhibited pDC differentiation. FLT3-ITD, CA-N-Ras, and TEL/PDGFRβ aberrantly induced programmed death ligand-1 (PD-L1)-expressing DCs. In conclusion, we have established a simple, efficient, and reproducible *in vitro* FL-DC differentiation system from LSKs. This system could uncover novel findings on how myeloid neoplasm-related gene abnormalities differentially affect FL-DC differentiation from murine hematopoietic stem/progenitor cells in a gene-specific manner.

1. Introduction

DCs are professional antigen-presenting cells, and are the only cell type that can prime naive T cells. Hence, DCs play a pivotal role in innate and adaptive immunities as well as tolerance [1,2]. There are at least two major subsets of DCs, cDCs and pDCs [3]. cDCs possess numerous dendrites and exhibit high expression of major histocompatibility complex class II (MHC II), thereby enabling the stimulation of naïve T cells in the presence of appropriate costimulation. By contrast, pDCs have no or few dendrites and exhibit a plasmacytoid round morphology and low expression of MHC II and costimulatory molecules. Therefore, pDCs are poor stimulators of naïve T cells.

In tumor immunology, deregulation of differentiation, maturation, and function of DCs is thought to contribute to the inhibition of anti-tumor immunity, thereby facilitating disease progression [4–6]. DCs in cancer tissue and cancer-draining lymph nodes often display an immature phenotype both in tumor-bearing animals and in patients with cancer [5–7]. These immature DCs are reported to often induce tolerance by presenting antigens to T cells [2,5,8]. Moreover, the immunosuppressive milieu created by tumors frequently causes a decrease in the numbers of cDCs with no or little effect on the numbers of pDCs, which are known to play important roles in the maintenance of tolerance [6,7]. It has also been shown in mouse models that tumors themselves produced tumor-specific tolerance by pDCs or cDCs through expression of indoleamine 2,3-dioxygenase (IDO) or PD-L1 (also called B7-H1), respectively [9,10]. Thus, DC abnormalities in malignant tumors are characterised by the deregulation of the maturation states, subsets, or functions of DCs.

In contrast to non-hematopoietic malignancies, leukemic cells from patients with acute myeloid leukemia (AML) can differentiate into DCs *ex vivo* in the presence of granulocyte macrophage colony-stimulating factor (GM-CSF) with or without interleukin (IL)-4 [11]. These cells retain leukemic gene abnormalities of the original leukemic cells, hence enabling presentation of known and potentially unknown leukemia-associated antigens (LAAs) [12]. Therefore, in the case of AML, leukemia-derived DCs *ex vivo* (*ex*

* Corresponding author. Tel.: +81 6 6879 3871; fax: +81 6 6879 3879.
E-mail address: mizuki@bldon.med.osaka-u.ac.jp (M. Mizuki).

0165-2478/$ – see front matter © 2011 Elsevier B.V. All rights reserved.
doi:10.1016/j.imlet.2010.12.006

vivo leukemic DCs), which are sometimes referred to as AML-DCs or AML-derived DCs, have been used in DC immunotherapy. In addition to *ex vivo* leukemic DCs, populations of spontaneously differentiated DCs *in vivo* from leukemic cells (*in vivo* leukemic DCs) exist in patients with AML [13,14], chronic myeloid leukemia (CML) [15], and myelodysplastic syndrome (MDS) [16,17]. Because DCs derived from normal cells *in vivo* (*in vivo* normal-origin DCs) are present in these patients, one must discriminate the three different types of DCs that may be present in cases of hematopoietic neoplasm: *in vivo* leukemic DCs, *in vivo* normal-origin DCs, and *ex vivo* leukemic DCs. Although *in vivo* leukemic DCs are thought to have LAAs [13,14] and postulated to affect anti-leukemia immune responses, there have been few reports detailing concise examinations about their subsets, maturation state, or function [13–17].

By contrast, much work has been done on *ex vivo* leukemic DCs [11,18], which are cultured in the presence of GM-CSF. However, the concentration of GM-CSF under steady-state conditions is low or undetectable and *in vitro* GM-CSF-mediated DCs (GM-DCs) are regarded as monocyte-derived DCs, which are induced only under *in vivo* inflammatory states [3,19]. By contrast, the FLT3 ligand (FL) is a crucial cytokine for steady-state DC development *in vivo*, and *in vitro* FL-mediated DCs (FL-DCs) are close equivalents to *in vivo* steady-state splenic DCs [3,19,20]. In patients with leukemia, steady-state conditions refer to the early phase of the disease or the phase of minimal residual disease after therapy. Therefore, it is important to examine the properties of *in vivo* leukemic DCs under steady-state conditions, which are postulated to affect host immune responses in a LAA-specific manner. In this study, we aimed to establish a culture method to induce FL-DCs from LSKs, which are the target for leukemic transformation. We selected FL as a cytokine to induce DCs *in vitro*, which is in contrast to previous studies that have used GM-CSF. This system enabled us to evaluate the direct effects of myeloid neoplasm-related gene abnormalities on FL-DC subsets, their maturation state, and function. Our results reveal novel functions of myeloid neoplasm-related gene abnormalities as direct immune modifiers.

2. Materials and methods

2.1. Mice

C57BL/6 mice (6–9 weeks of age) were used for DC cultures. BALB/c mice (10–13 weeks of age) were used for the mixed leukocyte reaction. All animals were maintained in a pathogen-free barrier facility and handled according to institutional guidelines.

2.2. Antibodies and flow cytometry

Single-cell suspensions were treated with an Fc receptor-blocking antibody (2.4G2, BD Biosciences, San Jose, CA). When Fc receptor blocking was inadequate, purified isotype control antibodies were added to 2.4G2. Cells were subsequently stained with monoclonal antibodies conjugated with fluorescein isothiocyanate (FITC), phycoerythrin (PE), allophycocyanin (APC) or phycoerythrin-Cy7 (PE-Cy7). Biotinylated antibodies were detected using FITC conjugated streptavidin. The following antibodies were purchased from BD Biosciences. Gr-1 (RB6-8C5), Mac-1 (M1/70), Ter119 (TER-119), CD3ε (145-2C11), B220 (RA3-6B2), CD11c (HL3), I-A^b (AF6-120.1), CD40 (3/23), CD80 (16-10A1), CD86 (GL1), NK1.1 (PK136), CD172a (Sirp-α, P84), biotin CD24 (M1/69), c-Kit (2B8), Sca-1 (Ly6A/E, D7). The antibodies specific for PDCA-1 (eBio129c) and PD-L1 (MIH5) were purchased from eBioscience (San Diego, CA). The antibody specific for CCR9 (FAB2160P) was purchased from R&D systems (Minneapolis, MN). FACS analysis and cell sorting were performed using the FACS Canto II (BD Biosciences) and the FACS Aria (BD Biosciences) machines respectively.

2.3. Isolation of LSKs

Bone marrow cells extracted from 6- to 9-week-old C57BL/6 mice were mixed with CD117 MicroBeads (Miltenyi Biotech, Germany), and then $CD117^+$ cells were isolated with the autoMACS Separator (Miltenyi Biotech). The cells were stained with PE-conjugated antibodies specific for the lineage (Gr-1, Mac-1, Ter119, CD3ε, and B220) markers, APC-conjugated c-Kit-, and PE-Cy7-conjugated Sca-1-monoclonal antibodies. After washing, the cells were resuspended in 7-amino-actinomycin (7-AAD) (Calbiochem, San Diego, CA)-containing buffer. The 7-AAD^- $lineage^-$ $Sca\text{-}1^+$ c-Kit^{high} cells were subsequently sorted using the FACS Aria (BD Biosciences). The purity of LSKs was consistently greater than 97%.

2.4. In vitro DC culture

Purified LSKs were cultured in a 48-well flat-bottom culture plate at a density of $4–10 \times 10^4$ cells/well in IMDM (GIBCO BRL, Grand Island, NY) containing 10% (vol/vol) fetal bovine serum (FBS), penicillin (100 units/ml, Nacalai Tesque, Kyoto, Japan), streptomycin (100 μg/ml, Nacalai Tesque, Kyoto, Japan), murine SCF (100 ng/ml, R&D), and murine TPO (100 ng/ml, R&D) at 37 °C in a humidified air containing 5% CO_2 (pre-culture phase, Fig. 1A). After 48 h, cells were washed, resuspended in IMDM (GIBCO) containing 10% FBS, murine FLT3-ligand (FL) (100 ng/ml, R&D), sodium pyruvate (1 mM, GIBCO), and 2-ME (100 μM, WAKO, Osaka, Japan), seeded in a 96-well round-bottom culture plate at a density of 3×10^3 cells/well, and cultured at 37 °C in a humidified air containing 10% CO_2 for the indicated period (DC-induction phase, Fig. 1A). In an *in vitro* GM-CSF/IL-4-mediated DC (GM/IL-4-DC) culture from LSKs, FL was substituted for GM-CSF (20 ng/ml, R&D) and IL-4 (10 ng/ml, R&D) during the DC-induction phase.

2.5. Plasmid constructs

Using the QuikChange™ Site-Directed Mutagenesis Kit (Stratagene, La Jolla, CA), we constructed a murine FLT3-internal tandem duplication (ITD) that contained a tandem insertion of Arg-Glu-Tyr-Glu-Asp-Lys between amino acids 602/603, similar with the previously reported FLT3-ITD [21]. The primer sequences for FLT3-ITD were as follows: 5′-agg-gaa-tat-gaa-gac-ctt-3′ (forward), 5′-aag-gtc-ttc-ata-ttc-cct-3′ (reverse). Murine FLT3 wild type (FLT3-WT) [22], murine FLT3-ITD, murine $FLT3^{Asp838Val}$ (FLT3-TKD) [22], N-$Ras^{Gly12Asp}$ (CA-N-Ras) [23], murine c-$Kit^{Asp814Val}$ (c-Kit-TKD) [24], FIP1L1/PDGFRα [25], TEL/PDGFRβ [25], AML1/ETO [26], PML/RARα [27], CBFβ/MYH11 [28], AML1dC [29] were each subcloned into a murine stem cell virus-internal ribosome entry site-EGFP (pMie) vector. pMYs-IRES-EGFP, a retrovirus expression vector, was kindly provided by Dr. T. Kitamura (University of Tokyo, Tokyo, Japan). STAT3c [30], 1*6-STAT5A [31], constitutive active form of MEK1 (CA-MEK1) (Invitrogen, Carlsbad, CA, USA), and membrane-targeted p110 [32] were each subcloned into pMYs-IRES-EGFP.

2.6. Preparation of retroviral particles

Conditioned medium containing high titer retroviral particles was prepared as reported previously with some modifications [33]. Briefly, each retroviral vector was cotransfected with vesicular stomatitis virus glycoprotein-, and gag/pol-expression plasmids into 293T cells by Lipofectamine 2000 (Invitrogen). After 48 h, the

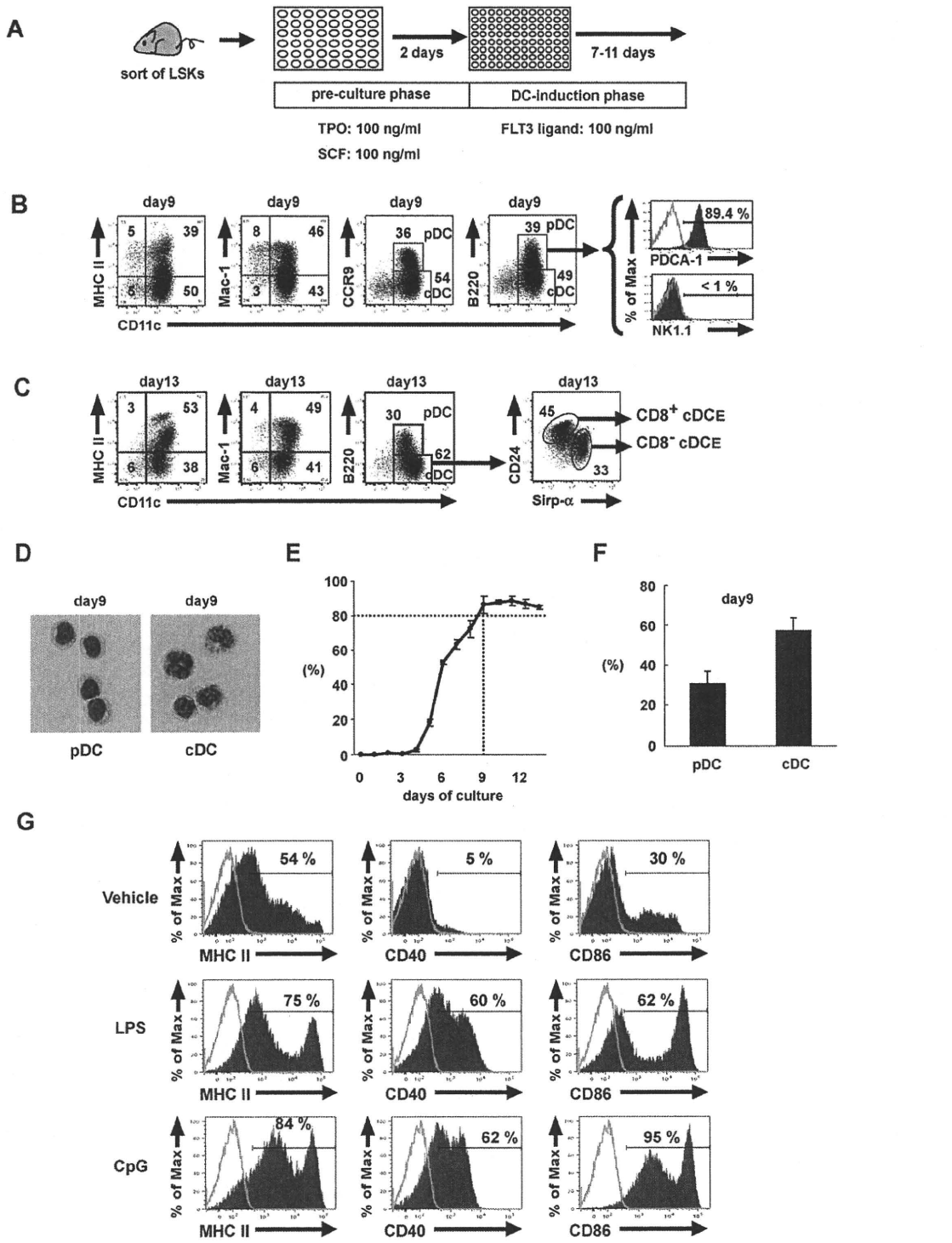

Fig. 1. FL-DCs from LSKs are phenotypically and morphologically similar to FL-DCs from whole bone marrow cells. (A) Schema of an *in vitro* FL-mediated DC differentiation system from LSKs. After 9 (B) or 13 (C) days of culture, cells were collected and the expression of the indicated surface markers was analysed by flow cytometry. (D) After 9 days in culture, FACS-sorted pDCs ($CD11c^+B220^+CCR9^+$) or cDCs ($CD11c^+B220^-CCR9^-$) cells were spun onto slides, and stained with May-Giemsa. Images are shown at ×400 original magnification. (E) Cells were harvested at the indicated day of culture and the surface expression of CD11c was analysed by flow cytometry. (F) After 9 days in culture, cells were collected and the expression of CD11c and B220 was analysed by flow cytometry. The bars show the proportion of pDCs ($CD11c^+B220^+$ cells) and cDCs ($CD11c^+B220^-$ cells) in cultured cells respectively. Numbers in the dot plots represent percentage of cells. (G) After 9 days in culture, cells were stimulated with CpG (1 μM), LPS (1 μg/ml), or left unstimulated. After 24 h, cultured cells were stained with the indicated surface markers and analysed by flow cytometry on the gated $CD11c^+$ cell population. Filled and open histograms show specific staining and back ground staining respectively.

culture supernatant was collected, concentrated 100-fold in volume, filtered (0.45 μm), and aliquoted for storage at −80 C until use.

2.7. Retroviral transduction into murine hematopoietic stem/progenitor cells

Purified LSKs were cultured in IMDM medium (GIBCO) containing 10% FBS, penicillin (100 unit/ml), streptomycin (100 μg/ml), murine SCF (100 ng/ml, R&D), and murine TPO (100 ng/ml, R&D) in a flat-bottom 48-well culture plate at 37 C in a humidified air containing 5% CO_2. After 24 h, cells were seeded into a flat-bottom 48-well culture plate coated with Retronectin (TAKARA BIO, Shiga, Japan) at a density of $1.5–2.0 \times 10^5$ cells/well, and then infected with each retrovirus in the same medium containing protamine sulphate (10 μg/ml, Sigma, St Louis, MO). The cells were cultured at 37 C in a humidified air containing 5% CO_2 for 24 h after which the cells were washed and subjected to the DC-induction phase.

2.8. Allogeneic mixed leukocyte reaction (MLR)

Varying numbers of FACS-sorted, irradiated (30 Gy) *in vitro* FL-mediated $CD11c^+$ or $EGFP^+CD11c^+$ cells were plated in a 96-well round-bottom culture plate with 5×10^4 BALB/c splenic $CD4^+$ T cells that were immunomagnetically selected using the $CD4^+$ T Cell Isolation Kit (Miltenyi Biotec). The purified $CD4^+$ T cells were suspended in a final volume of 150 μl RPMI 1640 (Nacalai Tesque) supplemented with 10% FBS, 2-ME (50 μM), penicillin (100 units/ml, Nacalai Tesque), streptomycin (100 μg/ml, Nacalai Tesque) prior to the mixing reaction. Cells were cultured for 4 days and pulsed with 1 μCi [^{3}H]-thymidine (Amersham Biosciences, Buckinghamshire, UK) per well during the last 16 h of culture. [^{3}H]-thymidine incorporation was measured on a β-plate counter.

2.9. ELISA

To evaluate IFN-α production, more than 97% of purified FL-DCs that were immunomagnetically selected with CD11c microbeads (Miltenyi Biotec), were cultured for 24 h at a density of 5×10^4 cells/200 μl in a 96-well round-bottom culture plate in IMDM medium supplemented with 10% FBS, penicillin (100 units/ml, Nacalai Tesque), streptomycin (100 μg/ml, Nacalai Tesque), 2-ME (50 μM), and sodium pyruvate (1 mM, GIBCO). Cells were stimulated with 1 μM of CpG-A-ODN (5′-ggTGCATCGATGCAgggggG-3′; small letters indicate bases with phosphorothioate-modified backbones), lipopolysaccharide (LPS) (Escherichia coli O55:B5, 1 μg/ml, Sigma, St Louis, MO), or vehicle. Cultured supernatants were assayed using an IFN-α ELISA Kit (R&D systems).

2.10. Cell count

All cultured cells in each well were harvested at 3 or 9 days of culture, and the absolute cell numbers and the proportion of $EGFP^+$ cells were analysed by flow cytometry. Fold increase in $EGFP^+$ cells was obtained by dividing the mean absolute cell numbers of $EGFP^+$ cells in 8 wells at 9 days of culture by the number at 3 days of culture. Data are shown as mean ± standard deviation (SD) from at least three independent assays.

2.11. Statistics

Data are shown as mean ± standard deviation (SD), and the Student *t*-test was used to compare two groups of samples.

3. Results

3.1. Establishment of an in vitro FL-mediated DC differentiation system from LSKs

Our initial aim was to establish a reproducible *in vitro* FL-mediated DC (FL-DC) differentiation system from LSKs for the purpose of assessing the influence of target genes on steady-state DC differentiation. *In vitro* FL-mediated $CD11c^+$ cells from LSKs were subdivided into $CD11c^+B220^+CCR9^+$ cells (pDC phenotype) and $CD11c^+B220^-CCR9^-$ cells (cDC phenotype) (Fig. 1B) [34–37]. $CD11c^+B220^+$ cells also express PDCA-1 but not NK1.1 [38], which is compatible with the pDC phenotype. Consistent with previous studies on FL-DCs from whole bone marrow cells [3,20], FL-DCs from LSKs did not express CD4 or CD8α (data not shown). Additionally $CD11c^+B220^-$ cells could be subdivided into $CD24^{high}CD11b^{low}Sirp\alpha^{low}$ ($CD8^+$ cDC_E) and $CD24^{low}CD11b^{high}Sirp\alpha^{high}$ ($CD8^-$ cDC_E) cells (Fig. 1C), equivalent with $CD8\alpha^+$ and $CD8^-$ cDCs found *in vivo* respectively [20]. FL-DCs from LSKs expressed none or low levels of other lineage markers such as Gr-1, Ter119, CD3ε, CD19, and NK1.1 (data not shown). FL-DCs from LSKs were morphologically compatible with the FL-DCs from whole bone marrow cells (Fig. 1D). After 9 days of culture, greater than 80% of cultured cells were consistently CD11c positive (Fig. 1E). In addition, the proportion of pDCs ($CD11c^+B220^+$ cells) and cDCs ($CD11c^+B220^-$ cells) were reproducibly consistent (pDCs; 30.4 ± 6.4%, cDCs; 57.1 ± 6.4%, pDCs/cDCs ratio; 0.55 ± 0.19) (Fig. 1F). Similar to a previous study using a DC culture from whole bone marrow cells [39], a maximal number of DCs was obtained after 9–10 days of culture (day 9: $7.1 \pm 2.8 \times 10^4$ cells/well), which is similar to the kinetics of FL-induced DC expansion *in vivo* [40]. We next sought to determine the maturation ability of FL-DCs from LSKs. FL-DCs was associated with the upregulation of MHC II and costimulatory molecules upon stimulation with LPS or CpG (Fig. 1G). Similar to *in vitro* DC cultures from whole bone marrow cells, $CD11c^+$ cells included many pre-DCs, defined as $CD11c^+$MHC II^- cells (Fig. 1B and G). Pre-DCs are considered late-stage precursors, and differentiate with a minimal number of divisions into exclusively DC subsets [41,42]. Consistent with this, almost all pre-DCs immediately differentiated into $CD11c^+$MHC II^+ cells after 24 h stimulation with CpG or LPS (Fig. 1G). Therefore, we classified all $CD11c^+$ cells, including pre DCs, as FL-DCs. The pDC/cDC ratio did not significantly differ between 9 and 13 days in culture, whereas the proportion of pre-DCs at 13 days of culture was decreased compared to the proportion of pre-DCs at 9 days in culture (Fig. 1B and C). These results were reproducible in at least four independent experiments.

3.2. FL-DCs from LSKs are functional

We next determined whether FL-DCs from LSKs were functional. FL-DCs from LSKs efficiently stimulated allogeneic $CD4^+$ T cells (Fig. 2A). FL-DCs from LSKs yielded a large amount of type I interferon upon CpG-stimulation (Fig. 2B). These results indicated that FL-DCs from LSKs were functionally competent DCs.

3.3. FL-DC differentiation from LSKs is deregulated in a myeloid neoplasm-related gene abnormality-specific manner

Mohty et al. reported the quantitative imbalance of *in vivo* DC subsets in patients with AML and divided the patients into three groups according to the proportion of pDCs and cDCs [13], however, the cause for this heterogeneity was unknown. AMLs have heterogeneous myeloid neoplasm-related gene abnormalities, that are termed class I and class II mutations, which contribute to deregulated signal transduction pathways and myeloid differentiation impairment respectively [43]. On the other hand, DC

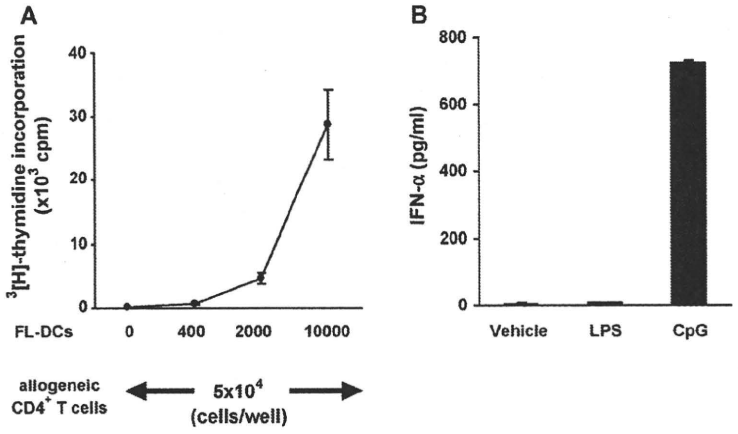

Fig. 2. FL-DCs from LSKs are functional. (A) Allogeneic CD4$^+$ T cells (5×10^4 cells) from BALB/c mice were co-cultured with graded numbers of irradiated (30Gy) FACS-sorted FL-DCs (CD11c$^+$ cells) from C57BL/6 mice for 4 days. Proliferation was measured by [^{3}H]-thymidine incorporation. Mean ± SD is shown. Experiments were repeated at least three times with similar results. (B) After 9 days in culture, FL-DCs were stimulated with CpG (1 μM), LPS (1 μg/ml), or left unstimulated in a total volume of 100 μl. After 24 h, the supernatants were harvested and assayed using ELISA.

differentiation is crucially regulated by STAT3/5 and in part associated with myeloid differentiation [3,44]. From these observations, we hypothesised that myeloid neoplasm-related gene abnormalities themselves might cause the quantitative imbalance found in *in vivo* leukemic DC subsets. Therefore, we determined whether myeloid neoplasm-related gene abnormalities affected FL-DC differentiation from LSKs. We selected FLT3-ITD, FLT3-TKD, CA-N-Ras, c-Kit-TKD, TEL/PDGFRβ, and FIP1L1/PDGFRα as representatives of class I mutations, and AML1/ETO, PML/RARα, CBFβ/MYH11, and AML1dC as representatives of class II mutations. We investigated how myeloid neoplasm-related gene abnormalities affected the absolute cell numbers of EGFP$^+$ cells (Fig. 3A). Compared with the mock population, all class I mutations except for FIP1L1/PDGFRα increased the number of EGFP$^+$ cells to various extents ($p < 0.01$). AML1/ETO and CBFβ/MYH11 yielded less EGFP$^+$ cells than mock population ($p < 0.05$). PML/RARα and AML1dC yielded comparable EGFP$^+$ cells to the mock population. We then focused on the proportion of whole FL-DCs (EGFP$^+$CD11c$^+$ cells in EGFP$^+$ cells). Compared to the mock population, all myeloid neoplasm-related gene abnormalities showed a significant decrease in the proportion of whole FL-DCs from LSKs ($p < 0.00001$) (Fig. 3B and C). Class II mutations uniformly displayed a mild decrease in the proportion of whole FL-DCs from LSKs (the proportion of EGFP$^+$CD11c$^+$ cells in EGFP$^+$ cells: 35.6–55.8%). By contrast, class I mutations exhibited variability (from mild to severe) in the decrease of the proportion of whole FL-DCs from LSKs (the proportion of EGFP$^+$CD11c$^+$ cells in EGFP$^+$ cells: 9.4–55.2%). From these data, we calculated the fold increase in whole FL-DC yields by multiplying the fold increase in EGFP$^+$ cells by the proportion of FL-DCs (the mean fold increase in EGFP$^+$ cells × the mean proportion of whole FL-DCs). FLT3-ITD and CA-N-Ras showed increased FL-DC yields than the mock population (Fig. 3D). The remaining class I mutations and all class II mutations exhibited decreased FL-DC yields. Lastly, we focused on the DC subsets, pDCs and cDCs. Compared with mock, CA-N-Ras, c-Kit-TKD, TEL/PDGFRβ, and FIP1L1/PDGFRα mutations displayed a severe decrease in the proportion of pDCs, with almost all EGFP$^+$CD11c$^+$ cells being cDCs, indicating a severe decrease in the pDC/cDC ratio (Fig. 3B and E). By contrast, FLT3-WT, FLT3-ITD, FLT3-TKD, and all class II mutations displayed comparable pDC/cDC ratios as the mock population. Taken together, class II mutations consistently yielded fewer FL-DCs from LSKs, and exhibited comparable pDC/cDC ratios with the control population. In contrast, class I mutations exhibited a variety of patterns regarding the whole FL-DC yields and their pDC/cDC ratios. FLT3-ITD and FLT3-TKD exhibited a comparable pDC/cDC ratio with the control, regardless of the difference in whole FL-DC yields. CA-N-Ras displayed a marked increase in the FL-DC yield and a severe decrease in the pDC/cDC ratio. c-Kit-TKD, TEL/PDGFRβ, and FIP1L1/PDGFRα exhibited less whole FL-DC yields and a severe decrease in the pDC/cDC ratio.

3.4. CA-N-Ras-, c-Kit-TKD-, TEL/PDGFRβ-, and FIP1L1/PDGFRα-expressing FL-DCs from LSKs showed distinct differentiation patterns from FL-DCs derived from LSKs

Two distinct types of DCs exist, steady-state and inflammatory DCs, the equivalents of which can be induced *in vitro* by FL or GM-CSF/IL-4 and are termed FL-DCs and GM/IL-4-DCs, respectively [3,19]. GM/IL-4-DCs are considered to be monocyte-derived DCs and composed of only cDCs. By contrast, FL-DCs include both pDCs and cDCs. Moreover, precursors of steady state DCs and FL-DCs are distinct from monocytes [19,45], suggesting that FL-DC and GM/IL-4-DC differentiation are distinct pathways. We focused on the differentiation pattern of FL-DCs and GM/IL-4-DCs from LSKs (Fig. 4A). In the presence of FL, almost all cultured cells began to express CD11c and Mac-1$^{-/dim}$ during 4–7 days in culture, and then they began to differentiate into CD11c$^+$Mac-1$^-$ and CD11c$^+$Mac-1$^+$ cells. In the presence of GM-CSF and IL-4, almost all cultured cells initially expressed Mac-1 and subsequently expressed CD11c after 7 days in culture. Consistent with previous reports, GM/IL4-DCs lacked pDCs (B220$^+$CD11c$^+$ cells) throughout the culture period (Fig. 4A). We next investigated the effects of CA-N-Ras, c-Kit-TKD, TEL/PDGFRβ, and FIP1L1/PDGFRα on the differentiation pattern of FL-DCs from LSKs (Fig. 4B). FL-DC differentiation from LSKs expressing CA-N-Ras, c-Kit-TKD, TEL/PDGFRβ, or FIP1L1/PDGFRα was characterised by the initial expression of Mac-1 during 4–7 days in culture, followed by the delayed expression of CD11c on Mac-1$^+$ cells. Among these four mutations, CA-N-Ras induced a significant proportion of CD11c$^+$Mac-1$^+$ cells at 7 days in culture. FL-DCs from LSKs expressing CA-N-Ras, c-Kit-TKD, TEL/PDGFRβ, or FIP1L1/PDGFRα generated few pDCs throughout the culture period.

3.5. Active forms of STAT5 and MEK1 severely impaired pDC differentiation from LSKs

We next examined why class I, but not class II, mutations caused variable patterns of FL-DC differentiation from LSKs. Class I, but not class II, mutations constitutively activated various sig-

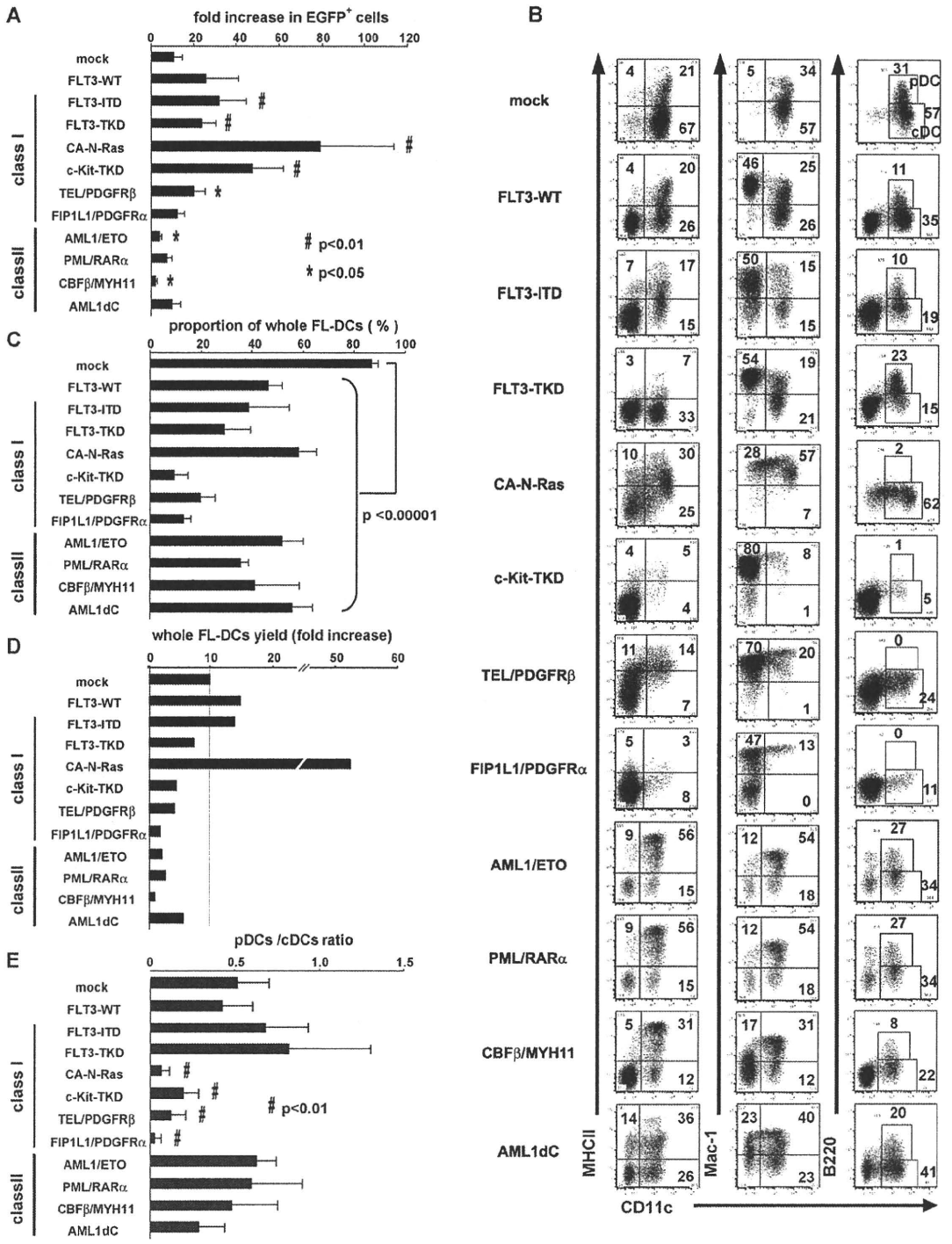

Fig. 3. FL-DC differentiation from LSKs is deregulated in a myeloid neoplasm-related gene abnormality-specific manner. During the pre-culture phase, cells were transduced with the indicated myeloid neoplasm-related gene abnormality. After 9 days in culture, cells were collected, and the absolute cell numbers and expressions of the indicated surface markers were analysed by gating on the EGFP$^+$ cells by flow cytometry (A–C, and E). Numbers in the dot plots represent percentage of cells. The bars represent fold increase in EGFP$^+$ cells (fold increase in absolute cell numbers of EGFP$^+$ cells from 3 to 9 days in culture) (A), the proportion of FL-DCs (EGFP$^+$CD11c$^+$ cells in EGFP$^+$ cells) (C), FL-DC yields (the mean fold increase in EGFP$^+$ cells × the mean proportion of whole FL-DCs) (D), and pDCs (EGFP$^+$CD11c$^+$B220$^+$ cells)/cDCs (EGFP$^+$CD11c$^+$B220$^-$ cells) ratio (E), respectively. Data are representative of at least three experiments with similar results. Mean ± SD is shown. * and # indicate $p < 0.05$ and $p < 0.01$ respectively.

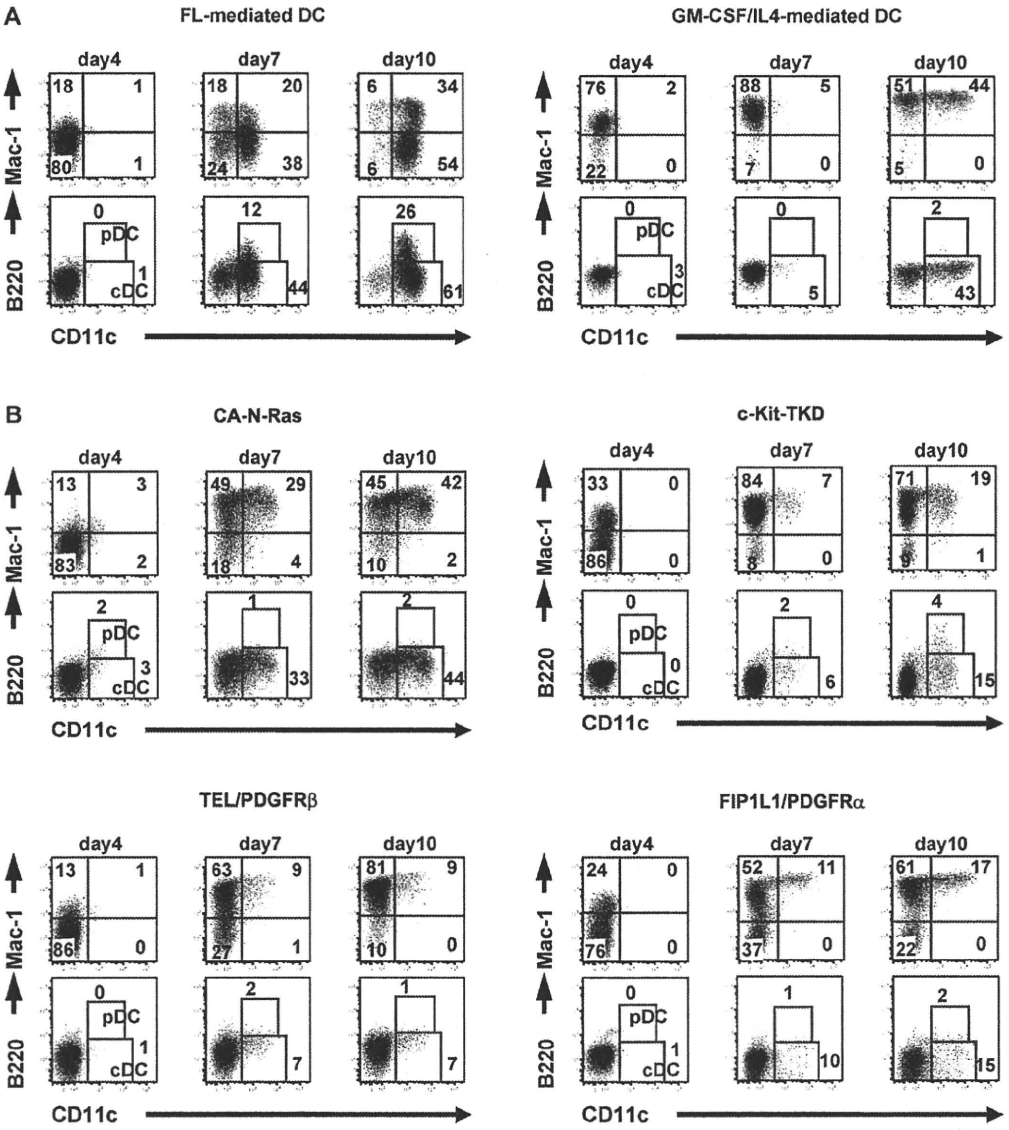

Fig. 4. CA-N-Ras-, c-Kit-TKD-, TEL/PDGFRβ-, and FIP1L1/PDGFRα-expressing FL-DCs from LSKs showed distinct differentiation patterns. (A) After the indicated days in culture in the presence of FL or GM-CSF with IL-4, cells were collected and the expression of the indicated surface markers was analysed by flow cytometry. (B) During the pre-culture phase, cells were transduced with the indicated myeloid neoplasm-related gene abnormality. After the indicated days of culture in the presence of FL, cells were collected and the expression of the indicated surface markers was analysed on the gated EGFP$^+$ cell population by flow cytometry. Numbers in the dot plots represent percentage of cells.

nal transduction pathways [43,46]. Therefore, we hypothesised that constitutively activated signals might generate the heterogeneous patterns of FL-DC differentiation from LSKs. We evaluated the influence of activated forms of signaling molecules on FL-DC differentiation from LSKs. We selected STAT3c, membrane-targeted p110, 1*6-STAT5A, and CA-MEK1 as a constitutively active form of STAT3, PI 3-kinase, STAT5, and MAP-kinase pathways, respectively. Compared with control cells, CA-STAT3 and CA-PI 3-kinase displayed a slight decrease in the proportion of whole FL-DCs from LSKs and was associated with a modest increase in the pDC/cDC ratio (Fig. 5). By contrast, CA-STAT5 and CA-MEK1 displayed a severe and mild decrease in the proportion of whole FL-DCs from LSKs, respectively. Both mutations resulted in a, severe decrease in the pDC/cDC ratio (Fig. 5).

3.6. Expression patterns of MHC II and costimulatory molecules on FL-DCs from LSKs are heterogeneous among class I mutations

We determined whether this heterogeneity in DC differentiation seen in class I mutations influenced the DC maturation state. DC maturation is associated with up-regulation of MHC II and costimulatory molecules [47]. We therefore screened the surface expression of MHC II and costimulatory molecules such as CD40, CD80, and CD86 on FL-DCs from LSKs bearing myeloid neoplasm-related gene abnormalities. Overall, expressions of MHC II, CD80, and CD86 on whole FL-DCs induced by class I mutations were higher than those in control cells with several exceptions such as MHC II expression on DCs induced by FLT3-TKD and FIP1L1/PDGFRα (Fig. 6A and B). None of the class I mutations induced expression

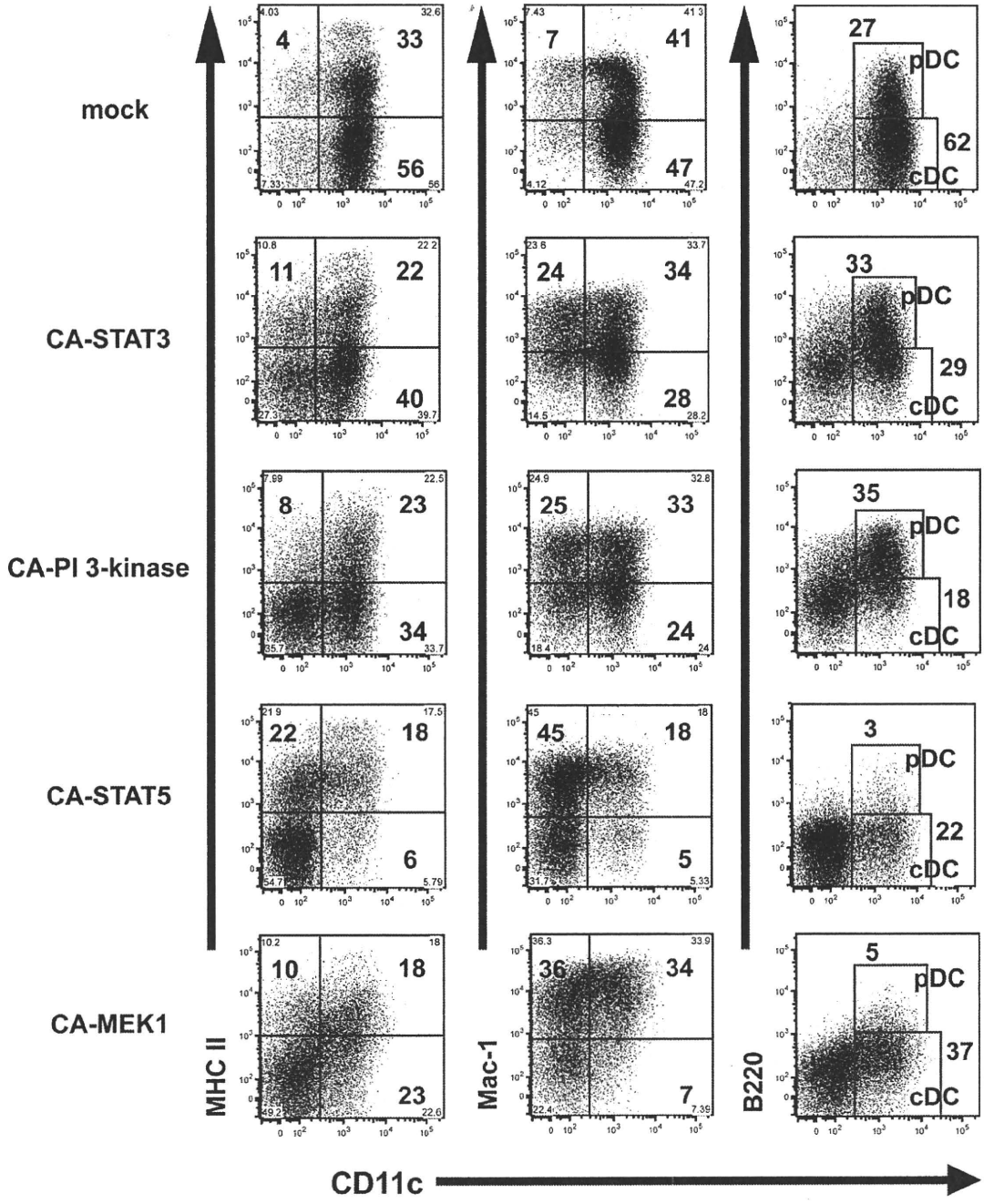

Fig. 5. Both active forms of STAT5 and MEK1 severely impaired pDC differentiation from LSKs. During the pre-culture phase, cells were transduced with the indicated activated form of signaling molecule. After 9 days in culture, cells were collected and the expression of the indicated surface markers was analysed by flow cytometry on the gated EGFP$^+$ cell population. Data are representative of at least two experiments with similar results. Numbers in the dot plots represent percentage of cells.

of CD40 on whole FL-DCs from LSKs (data not shown). In addition, we determined whether these differences in expression of MHC II and costimulatory molecules on FL-DCs from LSKs between class I mutations affected the ability to stimulate allogeneic CD4$^+$ T cells. Among class I mutations, we selected FLT3-ITD, CA-N-Ras, and TEL/PDGFRβ as representatives for an allogeneic MLR assay, because they showed contrasting patterns of whole FL-DC yields (Fig. 3D), pDC/cDC ratios (Fig. 3E), differentiation patterns (Fig. 4), and expression patterns of MHC II and costimulatory molecules (Fig. 6A and B). Both CA-N-Ras- and TEL/PDGFRβ-expressing FL-DCs from LSKs efficiently stimulated allogeneic CD4$^+$ T cells, possibly resulting from high expressions of MHC II and costimulatory molecules (Fig. 6C). By contrast, despite FLT3-ITD-expressing FL-DCs from LSKs exhibiting a relatively higher expression of MHC II and costimulatory molecules than those of mock cells, FLT3-ITD-expressing FL-DCs stimulated allogeneic CD4$^+$ T cells at comparable

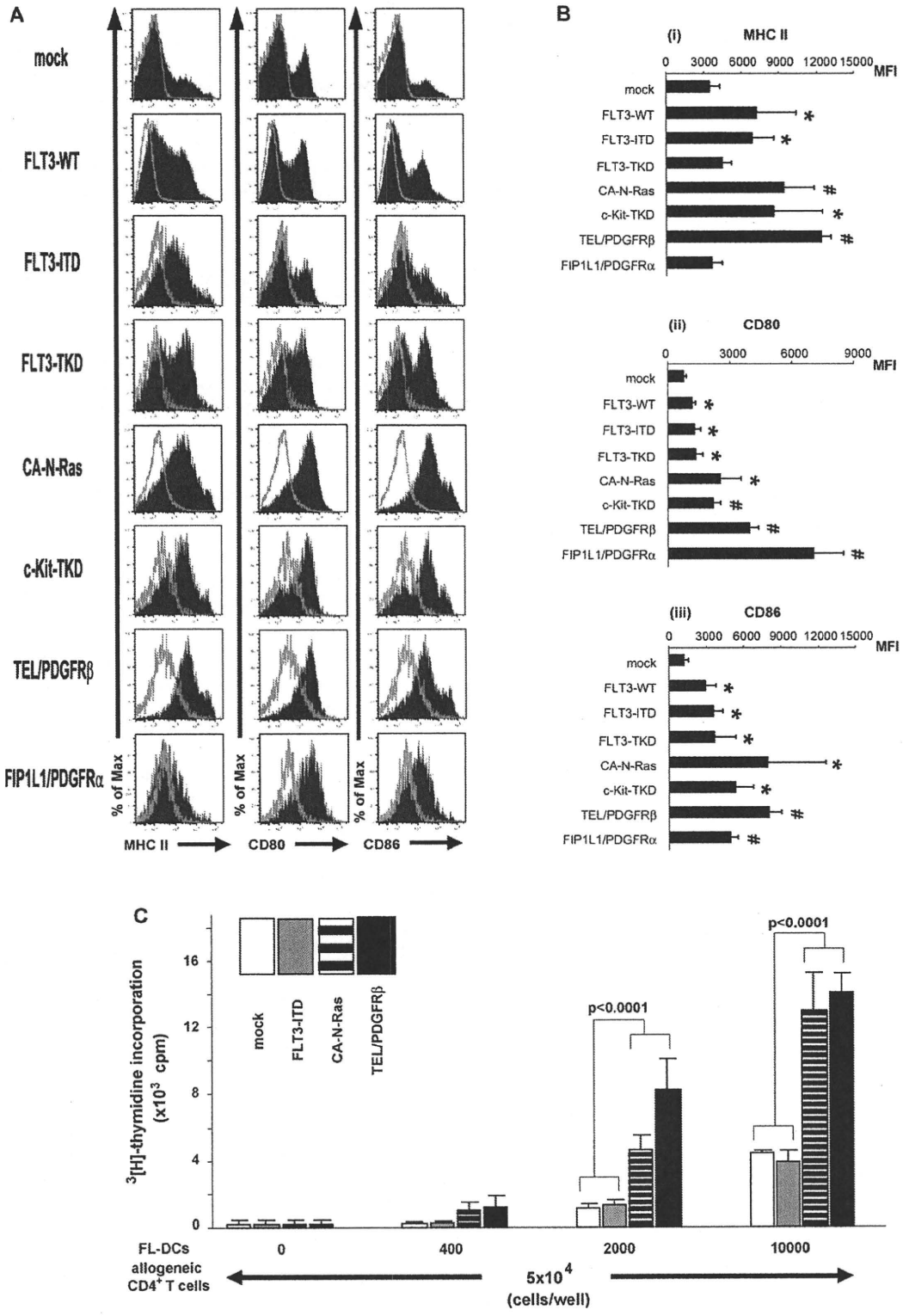

Fig. 6. Expression patterns of MHC II and costimulatory molecules on FL-DCs from LSKs are heterogeneous among class I mutations. During the pre-culture phase, cells were transduced with the indicated class I mutation. After 9 days in culture, cells were collected and the expression of MHC II and costimulatory molecules was analysed by flow cytometry on the gated EGFP⁺CD11c⁺ cell population. (A) Filled and open histograms show specific staining and back ground staining respectively. (B) The bars represent mean fluorescence intensity (MFI) of surface expression of MHC II (i), CD80 (ii), and CD86 (iii) respectively. (C) Allogeneic CD4⁺ T cells from BALB/c mice were co-cultured with graded numbers of irradiated (30 Gy) FACS-sorted EGFP⁺ FL-DCs from LSKs from C57BL/6 mice for 4 days. Proliferation was measured by [³H]-thymidine incorporation. Data are representative of at least three experiments with similar results. Mean ± SD is shown. * and # indicate $p < 0.05$ and $p < 0.01$ respectively.

level as control cells (Fig. 6C). Taken together, the class I mutations tested displayed heterogeneous expression patterns of MHC II and costimulatory molecules on FL-DCs from LSKs.

3.7. FLT3-ITD, CA-N-Ras, and TEL/PDGFRβ aberrantly induced PD-L1-expressing DCs

The interaction between programmed death-1 (PD-1) and PD-L1 results in diminished anti-tumor T-cell responses in both solid tumors [10,48–51] and hematological malignancies [52–54]. Therefore, we determined whether class I mutations induced expression of PD-L1 on FL-DCs from LSKs. We selected FLT3-ITD, CA-N-Ras, and TEL/PDGFRβ as representatives of class I mutations. FLT3-ITD, CA-N-Ras, and TEL/PDGFRβ induced PD-L1-expressing DCs, whereas the mock population did not induce PD-L1-expressing DCs (Fig. 7). In FLT3-ITD, CA-N-Ras, and TEL/PDGFRβ, the proportion of FL-DCs expressing PD-L1 was increased in an EGFP-intensity dependent manner, suggesting that the induction of PD-L1-expressing DCs correlated with the expression of each myeloid neoplasm-related gene abnormality.

4. Discussion

Little is known about *in vivo* DCs in patients with myeloid leukemia [13–17,55–57] compared with *ex vivo* leukemic DCs [11,18]. This may be a result from several obstacles in the study of *in vivo* DCs [58]. DCs are a relatively rare population *in vivo* compared with other hematopoietic cells [59]. In addition, the expression of aberrant markers such as CD7, CD19, or CD56 is often detected [60–62], and may be retained on *in vivo* leukemic DCs in AML cases. Therefore, it is difficult to phenotypically identify *in vivo* leukemic DCs, which are identified by the negative selection using surface markers such as CD3, CD14, CD16, CD19, and CD56 [13,16]. Furthermore, in hematological malignancies, two distinct types of DCs *in vivo* exist that differ in their origin, "*in vivo* leukemic DCs" and "*in vivo* normal-origin DCs". To date it is not possible to isolate viable *in vivo* leukemic DCs from *in vivo* normal-origin DCs until genetic analysis for leukemia-specific markers such as fluorescence *in situ* hybridisation, sequence, or polymerase chain reaction is performed. Thus, study into *in vivo* DCs in leukemia cases is challenging and may explain the relatively small number of studies that have investigated the significance of *in vivo* leukemic DCs.

In order to address this problem, we established a reproducible FL-mediated *in vitro* DC differentiation system from LSKs, which imitates the differentiation process of *in vivo* leukemic DCs. Our system is characterised by two points distinct from previous studies. First, the system recapitulates steady-state DC differentiation. In tumor immunology, once tolerance to tumor-associated antigens (TAAs) has been established, immunisation with TAA, even with the use of mature DCs merely enhances TAA-specific immunosuppression [63–66], suggesting that early TAA-specific immune responses critically affect subsequent tumor control. We believed it was important to analyse the properties of *in vivo* leukemic DCs during the early phase of the disease or at the phase of minimal residual disease after therapy, which is regarded as the steady-state condition in DC development. Therefore, in our DC differentiation system, we selected FL, a crucial cytokine in steady-state DC differentiation [3]. Second, we developed a DC differentiation system from murine LSKs, but not from whole bone marrow cells. Leukemic cells develop from hematopoietic stem cells or progenitor cells that have acquired various genetic abnormalities. These myeloid neoplasm-related gene abnormalities are characterised primarily as growth/survival promoting abnormalities or differentiation blocking abnormalities, and are described as class I or class II mutations, respectively [43]. These mutations classes have also been identified as prognostic factors, as demonstrated for FLT3-ITD [67,68]. Obviously, *in vivo* leukemic DCs should have the same origin and genetic abnormalities as leukemic blasts. Therefore, we transduced abnormal myeloid neoplasm-related abnormal genes into hematopoietic stem cells or progenitor cells (which are target cells for leukemic transformation) and subsequently induced these cells into DCs in the presence of FL. For this purpose, we used murine LSKs as the initial cell population for DC differentiation. At present, there is a well-established culture method to generate FL-DCs from whole bone marrow cells [19,20,39], which are equivalent with steady-state splenic DCs [3,19,20]. Because the cell density is important for this culture method [39], we selected a 96-well round-bottom rather than flat-bottom culture plate during the DC-induction phase to maintain a constant cell density. Consequently, we were able to establish a simple, efficient, and reproducible FL-DC differentiation system from LSKs without additional cytokines or feeder cells (Fig. 1A–F), thereby enabling a comparative study between various genetic manipulations.

In this study, we have found that class I mutations differentially affected FL-DC differentiation from LSKs regarding the fold increase in whole FL-DCs, and the pDC/cDC ratio (Fig. 3A–E). The effects of these mutations on FL-DC differentiation differed from those on myeloid differentiation, a process that is inhibited primarily by class II mutations [43]. A time course study of FL-DC differentiation showed that CA-N-Ras, c-Kit-TKD, TEL/PDGFRβ, and FIP1L1/PDGFRα induced a transition from Mac-1$^+$CD11c$^-$ to Mac-1$^+$CD11c$^+$ to varying degrees, which differed from the control FL-mediated DC differentiation pathway (Fig. 4A and B). These findings suggest that class I mutations deregulate FL-mediated DC differentiation or may convert it into GM-CSF/IL-4-mediated DC differentiation to various degrees despite the cells being cultured in the presence of FL. Previous studies showed that DC differentiation is regulated by FL and GM-CSF primarily through the activation of STAT3 via FLT3 and STAT5 via the GM-CSF receptor, respectively [3,69]. Thus, steady-state DC differentiation is composed of both pDCs and cDCs and is maintained by FL, of which activation of STAT3 is indispensable. By contrast, DC differentiation in the inflammatory state which produces only cDC, is mediated primarily by GM-CSF, in which the activation of STAT5 by GM-CSF plays an important role in promoting GM-CSF-mediated DC differentiation and inhibiting FL-mediated DC differentiation. In DC differentiation in the inflammatory state, activation of STAT3 is dispensable. In addition, it is postulated that FL- or GM-CSF-mediated DC differentiation is determined by the balance between the activations of STAT3 and STAT5 [69,70], which leads to the difference in pDC/cDC ratio. Consistent with these observations, CA-STAT5, but not CA-STAT3, impaired FL-DC, particularly pDC, differentiation in our system (Fig. 4). In addition, CA-MEK1 inhibited FL-DC, particularly pDC, differentiation. This inhibition is similar to that seen by CA-N-Ras, suggesting that the Ras/MAP kinase pathway plays a role in the impairment of pDC differentiation (Fig. 4). Because class I mutations constitutively and simultaneously activate multiple signal pathways [43], we speculate that these mutations differentially regulate FL-DC differentiation, possibly via their specific targets and extent of activation of each signal transduction pathway. Further studies will be required to investigate how each class I mutation and its deregulated signal transduction pathway is involved in FL-DC differentiation.

Mohty et al. [13] reported that patients with AML showed various patterns of quantitative imbalances in the proportions of circulating myeloid DCs (mDCs) (the human counterpart for murine cDCs) and pDCs. They classified these various patterns into three groups. Group I showed similar proportions with healthy volunteers. Group II included three subgroups: mDC expansion, pDC expansion, and mDC and pDC expansion. Group III showed no detectable DC subsets. The heterogeneous DC proportions in

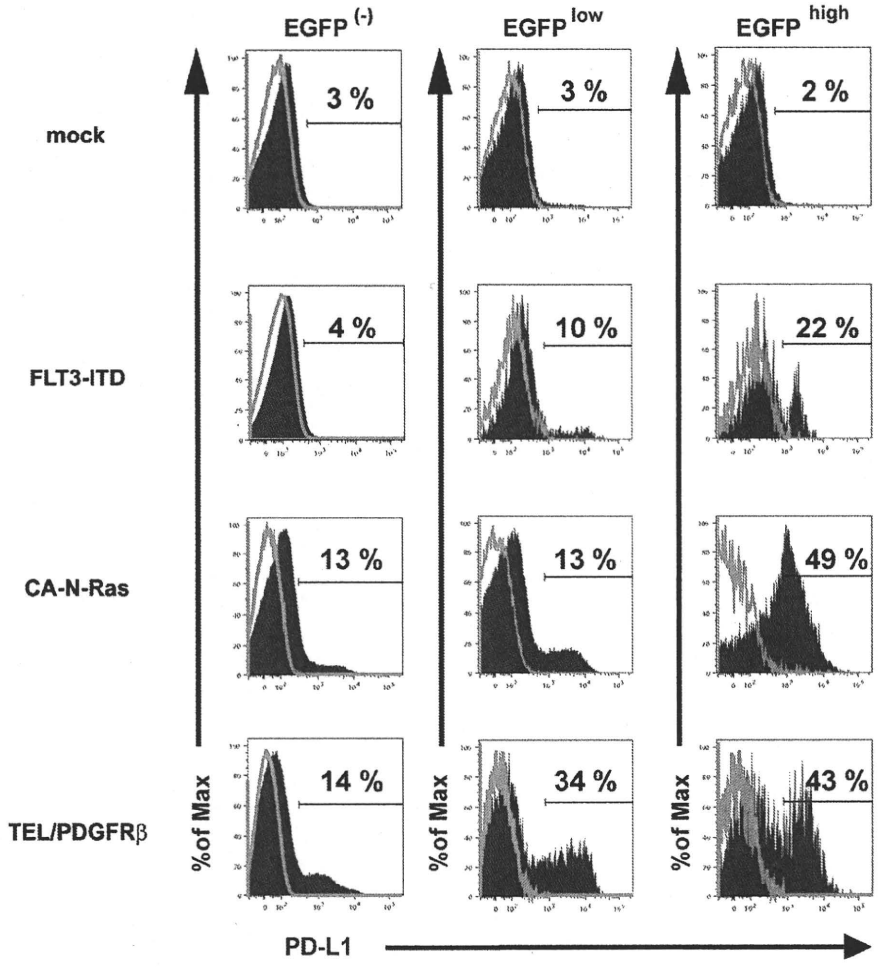

Fig. 7. FLT3-ITD, CA-N-Ras, and TEL/PDGFRβ aberrantly induce PD-L1-expressing DCs. During the pre-culture phase, cells were transduced with the indicated gene. After 9 days in culture, cells were collected and the expression of PD-L1 was analysed by flow cytometry on the gated EGFP$^-$CD11c$^+$, EGFP^{low}CD11c$^+$ and EGFP^{high}CD11c$^+$ cell population. Filled and open histograms show specific staining and back ground staining respectively. EGFP^{low} and EGFP^{high} cells were defined as those showing lower and higher fluorescence intensity than the MFI of all EGFP$^+$ cells, respectively. Data are representative of at least three experiments with similar results.

AML patients may partly reflect the various effects that myeloid neoplasm-related gene abnormalities have on DC differentiation as we have shown. However, particularly during the manifestation of the disease, *in vivo* DC differentiation may be affected by various mechanisms/factors such as abnormal secreted cytokine levels [7,56,71,72] and DC distributions [73]. Therefore, we should reassess the changes in *in vivo* DCs in relation to myeloid neoplasm-related gene abnormalities in patients with myeloid neoplasms.

DCs play a pivotal role in determining the balance between T cell immunity and tolerance to tumor cells [5,6,74]. Generally, mature and immature DCs contribute to T cell immunity and tolerance, respectively. pDCs usually display an immature phenotype and often facilitate tumor progression through various mechanisms [6,7,9] such as induction of T cell anergy or deletion, induction of T cells with regulatory property, IDO-mediated tryptophan catabolism, or induction of PD-L on IDO-negative DCs by IDO-positive pDCs. In this study, we have shown that FLT3-ITD specifically retained pDC differentiation from LSKs and showed relatively immature phenotype among class I mutations tested. In addition, FLT3-ITD aberrantly induced PD-L1-expressing DCs. Therefore, FLT3-ITD may work as an inducer of *in vivo* leukemic DCs with tolerogenic function among class I mutations, which may be one reason for it being a poor prognostic factor [67,68]. Therefore, whether leukemic DCs bearing FLT3-ITD have tolerogenic property needs to be further investigated. In contrast, both CA-N-Ras- and TEL/PDGFRβ-expressing FL-DCs exhibited a mature phenotype among the class I mutations tested and efficiently stimulated allogeneic T cells. Therefore, these mutations may have immunogenic properties. However, in certain immunological contexts, mature DCs can also contribute to tolerance by inducing T cells with regulatory properties [47,64]. In addition, both CA-N-Ras and TEL/PDGFRβ aberrantly induced PD-L1-expressing DCs. Therefore, how *in vivo* leukemic DCs bearing CA-N-Ras or TEL/PDGFRβ affect host immune responses needs to be further elucidated. In summary, the differentiation, maturation, and function of FL-DCs from LSKs are deregulated by myeloid neoplasm-related gene abnormalities, particularly class I mutations. Therefore, in patients with myeloid neoplasms, how myeloid neoplasm-related gene abnormalities (particularly class I mutations and associated deregulated signal transduction pathways), affect host immune system, tolerance and immunity, through *in vivo* leukemic DCs needs to be further examined. If *in vivo* leukemic DCs have tolerogenic prop-

erties, they may be candidate targets for therapy. Conversely, if *in vivo* leukemic DCs have immunogenic property, their inhibition may lead to disease progression.

In conclusion, here we have found the possible novel function inherent in myeloid neoplasm-related gene abnormalities, that is, the differentiation, maturation, and function of *in vivo* leukemic DCs may be differentially affected by myeloid neoplasm-related gene abnormalities themselves.

Acknowledgements

This work was supported by grants from the Ministry of Education, Science, Sports, and Culture and Technology of Japan. The authors thank Noriko Kikunaga and Yoko Habuchi for their professional assistance; Jun Ishiko, Isao Takahashi, Tetsuo Maeda, and Takafumi Yokota for their helpful advice and discussion.

References

[1] Banchereau J, Steinman RM. Dendritic cells and the control of immunity. Nature 1998;392:245–52.
[2] Steinman RM, Hawiger D, Liu K, Bonifaz L, Bonnyay D, Mahnke K, et al. Dendritic cell function in vivo during the steady state: a role in peripheral tolerance. Ann N Y Acad Sci 2003;987:15–25.
[3] Shortman K, Naik SH. Steady-state and inflammatory dendritic-cell development. Nat Rev Immunol 2007;7:19–30.
[4] Steinman RM, Banchereau J. Taking dendritic cells into medicine. Nature 2007;449:419–26.
[5] Dhodapkar MV, Dhodapkar KM, Palucka AK. Interactions of tumor cells with dendritic cells: balancing immunity and tolerance. Cell Death Differ 2008;15:39–50.
[6] Melief CJ. Cancer immunotherapy by dendritic cells. Immunity 2008;29:372–83.
[7] Gabrilovich D. Mechanisms and functional significance of tumour-induced dendritic-cell defects. Nat Rev Immunol 2004;4:941–52.
[8] Hawiger D, Inaba K, Dorsett Y, Guo M, Mahnke K, Rivera M, et al. Dendritic cells induce peripheral T cell unresponsiveness under steady state conditions in vivo. J Exp Med 2001;194:769–79.
[9] Sharma MD, Baban B, Chandler P, Hou DY, Singh N, Yagita H, et al. Plasmacytoid dendritic cells from mouse tumor-draining lymph nodes directly activate mature Tregs via indoleamine 2,3-dioxygenase. J Clin Invest 2007;117:2570–82.
[10] Curiel TJ, Wei S, Dong H, Alvarez X, Cheng P, Mottram P, et al. Blockade of B7-H1 improves myeloid dendritic cell-mediated antitumor immunity. Nat Med 2003;9:562–7.
[11] Houtenbos I, Westers TM, Ossenkoppele GJ, van de Loosdrecht AA. Feasibility of clinical dendritic cell vaccination in acute myeloid leukemia. Immunobiology 2006;211:677–85.
[12] Li L, Reinhardt P, Schmitt A, Barth TF, Greiner J, Ringhoffer M, et al. Dendritic cells generated from acute myeloid leukemia (AML) blasts maintain the expression of immunogenic leukemia associated antigens. Cancer Immunol Immunother 2005;54:685–93.
[13] Mohty M, Jarrossay D, Lafage-Pochitaloff M, Zandotti C, Briere F, de Lamballeri XN, et al. Circulating blood dendritic cells from myeloid leukemia patients display quantitative and cytogenetic abnormalities as well as functional impairment. Blood 2001;98:3750–6.
[14] Fujii S, Shimizu K, Koji F, Kawano F. Malignant counterpart of myeloid dendritic cell (DC) belonging to acute myelogenous leukemia (AML) exhibits a dichotomous immunoregulatory potential. J Leukoc Biol 2003;73:82–90.
[15] Orsini E, Calabrese E, Maggio R, Pasquale A, Nanni M, Trasarti S, et al. Circulating myeloid dendritic cell directly isolated from patients with chronic myelogenous leukemia are functional and carry the bcr-abl translocation. Leuk Res 2006;30:785–94.
[16] Ma L, Delforge M, van Duppen V, Verhoef G, Emanuel B, Boogaerts M, et al. Circulating myeloid and lymphoid precursor dendritic cells are clonally involved in myelodysplastic syndromes. Leukemia 2004;18:1451–6.
[17] Micheva I, Thanopoulou E, Michalopoulou S, Kakagianni T, Kouraklis-Symeonidis A, Symeonidis A, et al. Impaired generation of bone marrow CD34-derived dendritic cells with low peripheral blood subsets in patients with myelodysplastic syndrome. Br J Haematol 2004;126:806–14.
[18] Schmitt M, Casalegno-Garduno R, Xu X, Schmitt A. Peptide vaccines for patients with acute myeloid leukemia. Expert Rev Vaccines 2009;8:1415–25.
[19] Xu Y, Zhan Y, Lew AM, Naik SH, Kershaw MH. Differential development of murine dendritic cells by GM-CSF versus Flt3 ligand has implications for inflammation and trafficking. J Immunol 2007;179:7577–84.
[20] Naik SH, Proietto AI, Wilson NS, Dakic A, Schnorrer P, Fuchsberger M, et al. Cutting edge: generation of splenic CD8+ and CD8− dendritic cell equivalents in Fms-like tyrosine kinase 3 ligand bone marrow cultures. J Immunol 2005;174:6592–7.
[21] Spiekermann K, Bagrintseva K, Schwab R, Schmieja K, Hiddemann W. Overexpression and constitutive activation of FLT3 induces STAT5 activation in primary acute myeloid leukemia blast cells. Clin Cancer Res 2003;9:2140–50.
[22] Fenski R, Flesch K, Serve S, Mizuki M, Oelmann E, Kratz-Albers K, et al. Constitutive activation of FLT3 in acute myeloid leukaemia and its consequences for growth of 32D cells. Br J Haematol 2000;108:322–30.
[23] Delgado MD, Vaque JP, Arozarena I, Lopez-Ilasaca MA, Martinez C, Crespo P, et al. H-K- and N-Ras inhibit myeloid leukemia cell proliferation by a p21WAF1-dependent mechanism. Oncogene 2000;19:783–90.
[24] Hashimoto K, Matsumura I, Tsujimura T, Kim DK, Ogihara H, Ikeda H, et al. Necessity of tyrosine 719 and phosphatidylinositol 3′-kinase-mediated signal pathway in constitutive activation and oncogenic potential of c-kit receptor tyrosine kinase with the Asp814Val mutation. Blood 2003;101:1094–102.
[25] Stover EH, Chen J, Lee BH, Cools J, McDowell E, Adelsperger J, et al. The small molecule tyrosine kinase inhibitor AMN107 inhibits TEL-PDGFRbeta and FIP1L1-PDGFRalpha in vitro and in vivo. Blood 2005;106:3206–13.
[26] Shimizu K, Kitabayashi I, Kamada N, Abe T, Maseki N, Suzukawa K, et al. AML1-MTG8 leukemic protein induces the expression of granulocyte colony-stimulating factor (G-CSF) receptor through the up-regulation of CCAAT/enhancer binding protein epsilon. Blood 2000;96:288–96.
[27] Alcalay M, Tomassoni L, Colombo E, Stoldt S, Grignani F, Fagioli M, et al. The promyelocytic leukemia gene product (PML) forms stable complexes with the retinoblastoma protein. Mol Cell Biol 1998;18:1084–93.
[28] Zhao L, Cannons JL, Anderson S, Kirby M, Xu L, Castilla LH, et al. CBFB-MYH11 hinders early T-cell development and induces massive cell death in the thymus. Blood 2007;109:3432–40.
[29] Satoh Y, Matsumura I, Tanaka H, Ezoe S, Fukushima K, Tokunaga M, et al. AML1/RUNX1 works as a negative regulator of c-Mpl in hematopoietic stem cells. J Biol Chem 2008;283:30045–56.
[30] Bromberg JF, Wrzeszczynska MH, Devgan G, Zhao Y, Pestell RG, Albanese C, et al. Stat3 as an oncogene. Cell 1999;98:295–303.
[31] Matsumura I, Kitamura T, Wakao H, Tanaka H, Hashimoto K, Albanese C, et al. Transcriptional regulation of the cyclin D1 promoter by STAT5: its involvement in cytokine-dependent growth of hematopoietic cells. EMBO J 1999;18:1367–77.
[32] Doornbos RP, Theelen M, van der Hoeven PC, van Blitterswijk WJ, Verkleij AJ, van Bergen en Henegouwen PM. Protein kinase Czeta is a negative regulator of protein kinase B activity. J Biol Chem 1999;274:8589–96.
[33] Satoh Y, Matsumura I, Tanaka H, Ezoe S, Sugahara H, Mizuki M, et al. Roles for c-Myc in self-renewal of hematopoietic stem cells. J Biol Chem 2004;279:24986–93.
[34] Nakano H, Yanagita M, Gunn MD. CD11c(+)B220(+)Gr-1(+) cells in mouse lymph nodes and spleen display characteristics of plasmacytoid dendritic cells. J Exp Med 2001;194:1171–8.
[35] O'Keeffe M, Hochrein H, Vremec D, Caminschi I, Miller JL, Anders EM, et al. Mouse plasmacytoid cells: long-lived cells, heterogeneous in surface phenotype and function, that differentiate into CD8(+) dendritic cells only after microbial stimulus. J Exp Med 2002;196:1307–19.
[36] Nikolic T, Dingjan GM, Leenen PJ, Hendriks RW. A subfraction of B220(+) cells in murine bone marrow and spleen does not belong to the B cell lineage but has dendritic cell characteristics. Eur J Immunol 2002;32:686–92.
[37] Pelayo R, Hirose J, Huang J, Garrett KP, Delogu A, Busslinger M, et al. Derivation of 2 categories of plasmacytoid dendritic cells in murine bone marrow. Blood 2005;105:4407–15.
[38] Blasius AL, Barchet W, Cella M, Colonna M. Development and function of murine B220+CD11c+NK1.1+ cells identify them as a subset of NK cells. J Exp Med 2007;204:2561–8.
[39] Brasel K, De Smedt T, Smith JL, Maliszewski CR. Generation of murine dendritic cells from flt3-ligand-supplemented bone marrow cultures. Blood 2000;96:3029–39.
[40] Maraskovsky E, Brasel K, Teepe M, Roux ER, Lyman SD, Shortman K, et al. Dramatic increase in the numbers of functionally mature dendritic cells in Flt3 ligand-treated mice: multiple dendritic cell subpopulations identified. J Exp Med 1996;184:1953–62.
[41] Naik SH, Sathe P, Park HY, Metcalf D, Proietto AI, Dakic A, et al. Development of plasmacytoid and conventional dendritic cell subtypes from single precursor cells derived in vitro and in vivo. Nat Immunol 2007;8:1217–26.
[42] Naik SH. Generation of large numbers of pro-DCs and pre-DCs in vitro. Methods Mol Biol 2010;595:177–86.
[43] Gilliland DG, Griffin JD. The roles of FLT3 in hematopoiesis and leukemia. Blood 2002;100:1532–42.
[44] Waskow C, Liu K, Darrasse-Jeze G, Guermonprez P, Ginhoux F, Merad M, et al. The receptor tyrosine kinase Flt3 is required for dendritic cell development in peripheral lymphoid tissues. Nat Immunol 2008;9:676–83.
[45] Naik SH, Metcalf D, van Nieuwenhuijze A, Wicks I, Wu L, O'Keeffe M, et al. Intrasplenic steady-state dendritic cell precursors that are distinct from monocytes. Nat Immunol 2006;7:663–71.
[46] Scholl C, Gilliland DG, Frohling S. Deregulation of signaling pathways in acute myeloid leukemia. Semin Oncol 2008;35:336–45.
[47] Rutella S, Danese S, Leone G. Tolerogenic dendritic cells: cytokine modulation comes of age. Blood 2006;108:1435–40.
[48] Blank C, Brown I, Peterson AC, Spiotto M, Iwai Y, Honjo T, et al. PD-L1/B7H-1 inhibits the effector phase of tumor rejection by T cell receptor (TCR) transgenic CD8+ T cells. Cancer Res 2004;64:1140–5.

[49] Hirano F, Kaneko K, Tamura H, Dong H, Wang S, Ichikawa M, et al. Blockade of B7-H1 and PD-1 by monoclonal antibodies potentiates cancer therapeutic immunity. Cancer Res 2005;65:1089–96.
[50] Strome SE, Dong H, Tamura H, Voss SG, Flies DB, Tamada K, et al. B7-H1 blockade augments adoptive T-cell immunotherapy for squamous cell carcinoma. Cancer Res 2003;63:6501–5.
[51] Iwai Y, Ishida M, Tanaka Y, Okazaki T, Honjo T, Minato N. Involvement of PD-L1 on tumor cells in the escape from host immune system and tumor immunotherapy by PD-L1 blockade. Proc Natl Acad Sci U S A 2002;99:12293–7.
[52] Mumprecht S, Schurch C, Schwaller J, Solenthaler M, Ochsenbein AF. Programmed death 1 signaling on chronic myeloid leukemia-specific T cells results in T-cell exhaustion and disease progression. Blood 2009;114:1528–36.
[53] Zhang L, Gajewski TF, Kline J. PD-1/PD-L1 interactions inhibit antitumor immune responses in a murine acute myeloid leukemia model. Blood 2009;114:1545–52.
[54] Liu J, Hamrouni A, Wolowiec D, Coiteux V, Kuliczkowski K, Hetuin D, et al. Plasma cells from multiple myeloma patients express B7-H1 (PD-L1) and increase expression after stimulation with IFN-{gamma} and TLR ligands via a MyD88-, TRAF6-, and MEK-dependent pathway. Blood 2007;110:296–304.
[55] Mohty M, Isnardon D, Vey N, Briere F, Blaise D, Olive D, et al. Low blood dendritic cells in chronic myeloid leukaemia patients correlates with loss of CD34+/CD38− primitive haematopoietic progenitors. Br J Haematol 2002;119:115–8.
[56] Boissel N, Rousselot P, Raffoux E, Cayuela JM, Maarek O, Charron D, et al. Defective blood dendritic cells in chronic myeloid leukemia correlate with high plasmatic VEGF and are not normalized by imatinib mesylate. Leukemia 2004;18:1656–61.
[57] Floisand Y, Normann AP, Heim S, Lund-Johansen F, Tjonnfjord GE. High expression of CD7 on CD34+ cells is not linked to deletion of derivative chromosome 9 or lack of dendritic cells in chronic myeloid leukaemia. Scand J Clin Lab Invest 2008;68:93–8.
[58] Panoskaltsis N. Dendritic cells in MDS and AML—cause, effect or solution to the immune pathogenesis of disease? Leukemia 2005;19:354–7.
[59] Robinson SP, Patterson S, English N, Davies D, Knight SC, Reid CD. Human peripheral blood contains two distinct lineages of dendritic cells. Eur J Immunol 1999;29:2769–78.
[60] Reading CL, Estey EH, Huh YO, Claxton DF, Sanchez G, Terstappen LW, et al. Expression of unusual immunophenotype combinations in acute myelogenous leukemia. Blood 1993;81:3083–90.
[61] Bahia DM, Yamamoto M, Chauffaille Mde L, Kimura EY, Bordin JO, Filgueiras MA, et al. Aberrant phenotypes in acute myeloid leukemia: a high frequency and its clinical significance. Haematologica 2001;86:801–6.
[62] Bhushan B, Chauhan PS, Saluja S, Verma S, Mishra AK, Siddiqui S, et al. Aberrant phenotypes in childhood and adult acute leukemia and its association with adverse prognostic factors and clinical outcome. Clin Exp Med 2010;10:33–40.
[63] Zhou G, Drake CG, Levitsky HI. Amplification of tumor-specific regulatory T cells following therapeutic cancer vaccines. Blood 2006;107:628–36.
[64] Maksimow M, Miiluniemi M, Marttila-Ichihara F, Jalkanen S, Hanninen A. Antigen targeting to endosomal pathway in dendritic cell vaccination activates regulatory T cells and attenuates tumor immunity. Blood 2006;108:1298–305.
[65] Wei S, Kryczek I, Zou L, Daniel B, Cheng P, Mottram P, et al. Plasmacytoid dendritic cells induce CD8+ regulatory T cells in human ovarian carcinoma. Cancer Res 2005;65:5020–6.
[66] Munn DH, Mellor AL. Indoleamine 2,3-dioxygenase and tumor-induced tolerance. J Clin Invest 2007;117:1147–54.
[67] Schlenk RF, Dohner K, Krauter J, Frohling S, Corbacioglu A, Bullinger L, et al. Mutations and treatment outcome in cytogenetically normal acute myeloid leukemia. N Engl J Med 2008;358:1909–18.
[68] Yanada M, Matsuo K, Suzuki T, Kiyoi H, Naoe T. Prognostic significance of FLT3 internal tandem duplication and tyrosine kinase domain mutations for acute myeloid leukemia: a meta-analysis. Leukemia 2005;19:1345–9.
[69] Onai N, Manz MG. The STATs on dendritic cell development. Immunity 2008;28:490–2.
[70] Cohen PA, Koski GK, Czerniecki BJ, Bunting KD, Fu XY, Wang Z, et al. STAT3- and STAT5-dependent pathways competitively regulate the pan-differentiation of CD34pos cells into tumor-competent dendritic cells. Blood 2008;112:1832–43.
[71] Tao M, Li B, Nayini J, Andrews CB, Huang RW, Devemy E, et al. SCF, IL-1beta, IL-1ra and GM-CSF in the bone marrow and serum of normal individuals and of AML and CML patients. Cytokine 2000;12:699–707.
[72] Panoskaltsis N, Reid CD, Knight SC. Quantification and cytokine production of circulating lymphoid and myeloid cells in acute myelogenous leukaemia. Leukemia 2003;17:716–30.
[73] Mumprecht S, Claus C, Schurch C, Pavelic V, Matter MS, Ochsenbein AF. Defective homing and impaired induction of cytotoxic T cells by BCR/ABL-expressing dendritic cells. Blood 2009;113:4681–9.
[74] Sotomayor EM, Borrello I, Rattis FM, Cuenca AG, Abrams J, Staveley-O'Carroll K, et al. Cross-presentation of tumor antigens by bone marrow-derived antigen-presenting cells is the dominant mechanism in the induction of T-cell tolerance during B-cell lymphoma progression. Blood 2001;98:1070–7.

THE JOURNAL OF BIOLOGICAL CHEMISTRY VOL. 285, NO. 41, pp. 31774–31782, October 8, 2010

BCR-ABL but Not JAK2 V617F Inhibits Erythropoiesis through the Ras Signal by Inducing p21$^{CIP1/WAF1}$*[S]

Received for publication, February 28, 2010, and in revised form, July 24, 2010 Published, JBC Papers in Press, July 27, 2010, DOI 10.1074/jbc.M110.118653

Masahiro Tokunaga[‡], Sachiko Ezoe[‡§1], Hirokazu Tanaka[‡], Yusuke Satoh[‡], Kentaro Fukushima[‡], Keiko Matsui[‡], Masaru Shibata[‡], Akira Tanimura[‡], Kenji Oritani[‡], Itaru Matsumura[‡¶], and Yuzuru Kanakura[‡]

From the [‡]Department of Hematology and Oncology, Osaka University Graduate School of Medicine, 2-2 Yamada-oka, Suita, Osaka 565-0871, the [§]Medical Center of Translational Research, Osaka University Hospital, Suita, Osaka 565-0871, and the [¶]Division of Hematology, Department of Internal Medicine, Kinki University School of Medicine, Osaka-Sayama, Osaka 589-8511, Japan

BCR-ABL is a causative tyrosine kinase (TK) of chronic myelogenous leukemia (CML). In CML patients, although myeloid cells are remarkably proliferating, erythroid cells are rather decreased and anemia is commonly observed. This phenotype is quite different from that observed in polycythemia vera (PV) caused by JAK2 V617F, whereas both oncogenic TKs activate common downstream molecules at the level of hematopoietic stem cells (HSCs). To clarify this mechanism, we investigated the effects of BCR-ABL and JAK2 V617F on erythropoiesis. Enforced expression of BCR-ABL but not of JAK2 V617F in murine LSK (Lineage$^-$Sca-1^{hi}CD117^{hi}) cells inhibited the development of erythroid cells. Among several signaling molecules downstream of BCR-ABL, an active mutant of N-Ras (N-RasE12) but not of STAT5 or phosphatidylinositol 3-kinase (PI3-K) inhibited erythropoiesis, while N-RasE12 enhanced the development of myeloid cells. BCR-ABL activated Ras signal more intensely than JAK2 V617F, and inhibition of Ras by manumycin A, a farnesyltransferase inhibitor, ameliorated erythroid colony formation of CML cells. As for the mechanisms of Ras-induced suppression of erythropoiesis, we found that GATA-1, an erythroid-specific transcription factor, blocked Ras-mediated mitogenic signaling at the level of MEK through the direct interaction. Furthermore, enforced expression of N-RasE12 in LSK cells derived from p53-, p16^{INK4a}/p19^{ARF}-, and p21$^{CIP1/WAF1}$-null/wild-type mice revealed that suppressed erythroid cell growth by N-RasE12 was restored only by p21$^{CIP1/WAF1}$ deficiency, indicating that a cyclin-dependent kinase (CDK) inhibitor, p21$^{CIP1/WAF1}$, plays crucial roles in Ras-induced suppression of erythropoiesis. These data would, at least partly, explain why respective oncogenic TKs cause different disease phenotypes.

Oncogenic tyrosine kinases (TKs)[2] such as BCR-ABL, FLT3-ITD, and JAK2 V617F are known to confer growth and/or survival advantage on hematopoietic cells, thereby causing hematologic malignancies (1–3). These gene alterations are supposed to occur at the hematopoietic stem cell (HSC) level (3, 4). Although these oncogenic TKs activate common downstream pathways including Ras/Raf/MEK/ERK, PI3-K/Akt, and STAT (1, 2, 5), their disease phenotypes are quite different: BCR-ABL is a causative gene of chronic myelogenous leukemia (CML) (1), FLT3-ITD of acute myeloid leukemia (AML) (2), and JAK2 V617F of myeloproliferative neoplasms including polycythemia vera (PV), essential thrombocythemia (ET) and primary myelofibrosis (PMF) (3). In patients with chronic-phase CML, anemia is a common feature in contrast to the marked leukocytosis in the peripheral blood. Also, bone marrow (BM) examination shows that erythroid islands are reduced in number and size despite the increased cellularity due to the granulocytic proliferation (6). This disease phenotype is totally different from that of PV, in which JAK2 V617F causes erythrocytosis together with the mild leukocytosis and thrombocytosis. Furthermore, in blast-phase CML, blast lineages are generally myeloid or lymphoid, and erythroid crisis is a rare incidence with a frequency no more than 5% (7, 8). These data suggest that, in contrast to the trilinear promoting activities of JAK2 V617F, BCR-ABL might not support the development of erythroid cells.

BCR-ABL activates several downstream pathways including Ras/Raf/MEK/ERK, STAT5, and PI3-K/Akt pathways (1, 4). Among them, we have previously shown that Ras plays crucial roles in the growth and survival of BCR-ABL-positive K562 cells, while STAT5 and PI3-K pathways contribute to their growth and survival to the only limited extent (9). In addition, although the role of STAT5 in BCR-ABL-mediated leukemogenesis remains controversial (10, 11), another group also reported that transformation of murine BM cells by BCR-ABL is blocked by dominant-negative Ras (12). Furthermore, Ras signaling was shown to be indispensable for the pathogenesis of CML in a murine BM transplantation model (13). Therefore, the activated Ras is considered to be essential for the pathogenesis of CML, and is also speculated to principally determine the disease phenotype of CML, that is, prominent proliferation of myeloid cells accompanied by the suppressed erythropoiesis.

* This work was supported by grants from the Ministry of Education, Science, Sports, and Culture and Technology of Japan.
[S] The on-line version of this article (available at http://www.jbc.org) contains supplemental Table S1 and Methods.
[1] To whom correspondence should be addressed. Tel.: 81-6-6879-3871; Fax: 81-6-6879-3879; E-mail: sezoe@bldon.med.osaka-u.ac.jp.
[2] The abbreviations used are: TK, tyrosine kinase; CML, chronic myelogenous leukemia; PV, polycythemia vera; HSC, hematopoietic stem cell; LSK, Lineage$^-$Sca-1^{hi}CD117^{hi}; BM, bone marrow; CDK, cyclin-dependent kinase; rh, recombinant human; TPO, thrombopoietin; rm, recombinant murine; EPO, erythropoietin; SCF, stem cell factor; G1ERT, GATA-1/ERT; 4-HT, 4-hydroxytamoxifen; Ab, antibody; HPRT, hypoxanthine phosphoribosyl transferase; pRb, retinoblastoma protein; PRAK, p38-regulated/activated protein kinase.

Ras is constitutively activated by various oncogenic TKs or mutations of Ras itself in various malignant tumors. Although oncogenic (or constitutively activated) Ras was originally shown to transmit mitogenic and survival signals through Raf/MEK/ERK (14), recent studies have demonstrated that, like other oncogenic stimuli, it also induces growth inhibition/arrest in normal cells to prevent their malignant transformation. In general, this biological phenomenon is called "cellular senescence" and observed in various types of non-hematopoietic cells (15, 16). In addition, excessive Ras signaling was reported to inhibit erythropoiesis (17, 18), indicating the presence of a similar cellular response in hematopoietic cells. So far, oncogenic Ras has been shown to cause senescence through several signaling pathways other than Raf/MEK/ERK (15, 19–21). Also, several cell cycle regulatory molecules such as p53, p16^{INK4a}, p19^{ARF} and p21$^{CIP1/WAF1}$, have been shown to play central roles in oncogene-induced senescence (15, 19, 21).

In this report, we found that BCR-ABL but not JAK2 V617F, and among their downstream molecules, Ras but not STAT5 or PI3-K suppress erythropoiesis from murine LSK cells. As for this mechanism, we found that an erythroid-lineage specific transcription factor, GATA-1, blocks Ras-dependent growth and survival by inhibiting MEK1 activity through the direct interaction. Furthermore, we showed that a cyclin-dependent kinase (CDK) inhibitor, p21$^{CIP1/WAF1}$, plays crucial roles in Ras-induced suppression of erythropoiesis using p21$^{CIP1/WAF1}$-deficient hematopoietic cells.

EXPERIMENTAL PROCEDURES

Cytokines and Reagents—Recombinant human thrombopoietin (rhTPO) and recombinant murine interleukin-3 (rmIL-3) were provided by Kyowa Hakko Kirin (Tokyo, Japan). Recombinant human erythropoietin (rhEPO) and murine stem cell factor (rmSCF) were purchased from R & D Systems (Minneapolis, MN). Manumycin A was purchased from Merck KGaA (Darmstadt, Germany).

Plasmid Constructs and cDNAs—Expression vectors for GATA-1/ERT (G1ERT) and wild-type (WT) GATA-1 were described previously (22). Active forms of N-Ras (N-RasE12) (23) and STAT5A (1*6 STAT5A) (24), and membrane-targeted PI3-K catalytic subunit (p110^{CAAX}) (25) were subcloned into pMYs-IRES-EGFP, a retrovirus expression vector, which was kindly provided by Dr. T. Kitamura (University of Tokyo, Tokyo, Japan). pMSCV-IRES-GFP-p210-BCR-ABL is a generous gift from Dr. C. J. Eaves (Terry Fox Laboratory, Vancouver, BC, Canada) (26). The cDNA of JAK2 V617F was kindly provided by Dr. K. Shimoda (University of Miyazaki, Miyazaki, Japan) (27) and was subcloned into pMSCV-IRES-GFP.

Cell Lines and Cultures—A murine IL-3-dependent hematopoietic cell line, Ba/F3, was maintained in RPMI (nacalai tesque, Kyoto, Japan) supplemented with 10% fetal bovine serum (FBS) (Equitech-Bio, Kerrville, TX) and 0.3 ng/ml rmIL-3. NIH3T3 and 293T cells were cultured in Dulbecco's modified Eagle's medium (DMEM; nacalai tesque) supplemented with 10% FBS.

Preparation of Stable Transformants from Ba/F3—We introduced G1ERT into Ba/F3 cells by electroporation (250 V and 950 microfarads) and selected stably transfected clones by the culture with G-418 (1.0 mg/ml; Wako Pure Chemical Industries, Osaka, Japan). We further introduced pMYs-IRES-EGFP-N-RasE12 and obtained doubly transfected clones by sorting GFP-positive cells with BD FACSAria Cell-Sorting System (BD Biosciences, San Jose, CA). Their IL-3-independent growth and cell cycle were analyzed with or without the activation of GATA-1 by 4-hydroxytamoxifen (4-HT; Sigma-Aldrich). DNA contents of the cells were evaluated by staining with propidium iodide.

Luciferase Assays—Luciferase assays were performed with a Dual-Luciferase Reporter Assay System (Promega, Madison, WI) as previously described (22). As for assays using Ba/F3 cells, transfection was performed with Amaxa Nucleofector technology (Lonza, Cologne, Germany), followed by the measurement of luciferase activities after 24 h.

Immunoblotting and Coimmunoprecipitation Analyses—Preparation of cell lysates, immunoprecipitation, gel electrophoresis, and immunoblotting were performed according to the methods described previously (22, 28). Antibodies (Abs) and reagents were supplied by the manufacturers described in supplemental methods.

Glutathione S-transferase (GST) Pull-down Assays—GST pull-down assays were performed as previously reported (22).

Animals—The congenic C57BL/6J mice were purchased from Clea Japan, Inc. (Tokyo, Japan). B6.129-Cdkn2a^{tm1Rdp} (p16^{INK4a}/p19^{ARF}-null) mice and p53-null mice were kindly provided by Technology Transfer Center National Cancer Institute (Rockville, MD) and Dr. N. Nishimoto (Wakayama Medical University, Wakayama, Japan), respectively. B6.129S2-Cdkn1a^{tm1Tyj}/J (p21$^{CIP1/WAF1}$-null) mice were purchased from The Jackson Laboratory (Bar Harbor, ME). The experimental designs of this study were approved by the Institutional Animal Care and Use Committee at Osaka University Graduate School of Medicine.

Separation of Murine Hematopoietic Progenitors—Murine BM cells were flushed from both femora and tibiae, and progenitors were concentrated by anti-mouse CD117 MicroBeads and autoMACS Pro Separator (Miltenyi Biotec, Bergisch Gladbach, Germany). To isolate LSK (Lineage$^-$Sca-1^{hi}CD117^{hi}) cells, selected progenitors were stained with phycoerythrin-conjugated (PE-conjugated) monoclonal Abs against murine lineage markers (CD3e (145–2C11), CD45R/B220 (RA3–6B2), Gr-1 (RB6–8C5), CD11b (M1/70), and TER-119 (TER-119)), fluorescein isothiocyanate-conjugated (FITC-conjugated) anti-Sca-1 Ab (E13–161.7), and allophycocyanin-conjugated (APC-conjugated) anti-CD117 Ab (2B8), and isolated by FACSAria. All Abs were purchased from BD Biosciences.

Preparation of Retrovirus Particles—Preparation of retrovirus particles was performed as described previously (29) (see supplemental methods).

Retrovirus Transfection into Murine BM Progenitors—Isolated LSK cells were precultured overnight in DMEM supplemented with 10% FBS, rmSCF (100 ng/ml), and rhTPO (100 ng/ml). Then, the cells were seeded on 24-well tissue plates coated with RetroNectin (TaKaRa Bio Inc., Shiga, Japan), infected with each viral supernatant by spinoculation, and cultured in the same medium containing 10% FBS, protamine sulfate (10 μg/ml; Sigma-Aldrich), rmSCF (50 ng/ml), and rhTPO (50 ng/ml). After 48 h of culture, retrovirus-transduced GFP$^+$

cells were sorted with FACSAria and were subjected to colony assays or stromal coculture.

Colony Assays—Cells were plated at the indicated density in methylcellulose medium (MethoCult; Stem Cell Technologies, Vancouver, BC, Canada) supplemented with the indicated growth factors. Cells were incubated with 5% CO_2 at 37 °C, and the numbers of colonies were counted after the indicated days.

Stromal Coculture—A murine BM stromal cell line, MS-5, was cultured in minimum essential medium (MEM) α (Invitrogen, Carlsbad, CA) with 10% FBS and prepared in 24-well tissue plates 1 day before the seeding. The sorted GFP$^+$ progenitors were seeded (1.5×10^3 cells/well) on the monolayer of MS-5 and cocultured in 2 ml of MEMα supplemented with 10% FBS, rmSCF (50 ng/ml), and rhEPO (3 units/ml). Five days after the initiation of coculture, hematopoietic cells were harvested and stained with PE-conjugated anti-CD45 (30-F11) Ab, and APC-conjugated anti-CD11b (M1/70) or anti-TER-119 (TER-119) Ab (all of them from BD Biosciences). To evaluate the phosphorylation status of ERK1/2, we used BD Phosflow technology (BD Biosciences). The harvested cells were further incubated in DMEM containing 2% FBS without cytokines for 4 h, then fixed, permeabilized, and stained with Alexa Fluor®647-conjugated anti-ERK1/2 (pT202/pY204) Ab (BD Biosciences) according to the manufacturer's recommendation.

Flow Cytometric Analyses—Flow cytometric analyses were performed using BD FACSCanto II (BD Biosciences). The data analyses were done with BD FACSDiva software (BD Biosciences) or FlowJo software (TreeStar, Ashland, OR).

Immunofluorescence Microscopy—5×10^4 of the transduced cells were cytospun onto microscope slides, fixed in 2% paraformaldehyde, and permeabilized in 1% Nonidet P-40 in PBS. After the incubation in blocking buffer (1 mg/ml of γ-globulin in PBS), the slides were incubated with a monoclonal Ab against p16^{INK4a} (F-12) or p19^{ARF} (5-C3-1) (both from Santa Cruz Biotechnology, Santa Cruz, CA). The slides were then incubated with an Alexa Fluor®546-conjugated secondary antibody (goat anti-mouse IgG for p16^{INK4a}, or goat anti-rat IgG for p19^{ARF}), followed by the staining of nuclei with Hoechst 33342 (all from Invitrogen). The slides were mounted in Fluoromount (Diagnostic BioSystems, Pleasanton, CA) before viewing on a LSM 5 PASCAL microscope (Carl Zeiss, Oberkochen, Germany).

Semiquantitative RT-PCR—Total RNA was isolated from 5×10^3 of the transduced cells using RNeasy Mini Kit (Qiagen, Hilden, Germany) and converted to cDNA by SuperScript III First Strand Synthesis System (Invitrogen). PCR was performed using Ampli Taq Gold (Applied Biosystems, Carlsbad, CA) with primers described in supplemental Table S1.

Real-time RT-PCR—Quantitative real-time RT-PCR was performed using FastStart Universal SYBR Green Master (Roche Diagnostics GmbH, Mannheim, Germany) and PRISM 7900HT (Applied Biosystems). Amplified signals were normalized to the levels of hypoxanthine phosphoribosyl transferase (HPRT). The primer sequences are described in supplemental Table S1.

BM Samples from CML Patients—BM samples were obtained from three patients with newly diagnosed chronic-phase CML. CD34$^+$ cells were separated using the MACS immunomagnetic separation system, and were subjected to colony assays. All BM samples were obtained after receiving written informed consent in accordance with the Declaration of Helsinki, and this study protocol was approved by the institutional review board of Osaka University Hospital.

Statistical Methods—Statistical analyses were carried out by standard Student *t* tests. Error bars used throughout indicate S.D.

RESULTS

BCR-ABL but Not JAK2 V617F Inhibits the Development of Erythroid Cells—To examine the effects of BCR-ABL on erythropoiesis, we first introduced p210-BCR-ABL into murine LSK cells using the retrovirus vector harboring GFP as a reporter gene. After 48 h, GFP$^+$ cells were sorted and cocultured with a murine BM stromal cell line, MS-5, in the presence of rmSCF and rhEPO for 5 days. As compared with mock-transduced cells, the proportion of CD45^{low}TER-119$^+$ erythroid cells was reduced in BCR-ABL-transduced cells significantly (Fig. 1*A*). We also examined the effects of JAK2 V617F on erythropoiesis with the same strategy and found that JAK2 V617F did not reduce the proportion of erythoroid cells. In colony assays, BCR-ABL significantly decreased the number of burst-forming units-erythroid (BFU-E), while it increased the number of myeloid colonies (Fig. 1*B*). On the other hand, JAK2 V617F did not reduce the number of BFU-E. These data indicate that BCR-ABL but not JAK2 V617F inhibits the development of erythroid cells from murine hematopoietic progenitors.

Oncogenic Ras Inhibits Erythropoiesis Downstream of BCR-ABL—BCR-ABL activates mainly Ras/Raf/MEK/ERK, JAK2/STAT5, and PI3-K/Akt pathways. Next, to examine the roles of these pathways in erythropoiesis, we transduced LSK cells with an active form of each signal transduction molecule: N-RasE12 for an active form of N-Ras, 1*6 STAT5A for STAT5, and p110^{CAAX} for PI3-K. Compared with Mock, 1*6 STAT5A and p110^{CAAX} increased total erythroid cell numbers by 2.8- and 1.9-fold, respectively (both, $p < 0.05$), while the proportion of erythroid cells was scarcely influenced by both molecules due to the increase in total cell numbers (Fig. 2, *A* and *B*). In contrast, N-RasE12 remarkably reduced not only the frequency (Fig. 2*A*) but also the number of erythroid cells (0.28-fold) (Fig. 2*B*), while it significantly increased the number of CD11b$^+$-myeloid cells (Fig. 2*C*). We also performed colony assays using N-RasE12- or Mock-transduced LSK cells. As shown in Fig. 2*D*, N-RasE12 significantly reduced the number of BFU-E (average colony numbers from 1.0×10^3 cells input: Mock-transduced cells, 9.7; N-Ras-transduced cells, 0.33) ($p < 0.01$).

BCR-ABL Activates Ras Signal More Intensely than JAK2 V617F—Next, we tried to clarify why JAK2 V617F did not suppress erythropoiesis, because it has been reported to activate Ras as well as BCR-ABL (5). For this purpose, we introduced JAK2 V617F and BCR-ABL into murine LSK cells, cocultured them with MS-5, and evaluated the Ras activity by expediently measuring the phosphorylation status of ERK1/2 after 4-h starvation of cytokines. As shown in Fig. 2*E*, ERK1/2 was more intensely phosphorylated (activated) in cells transduced with BCR-ABL than in those with JAK2 V617F. We also examined the phosphorylation status of ERK1/2 in CML patients' blood

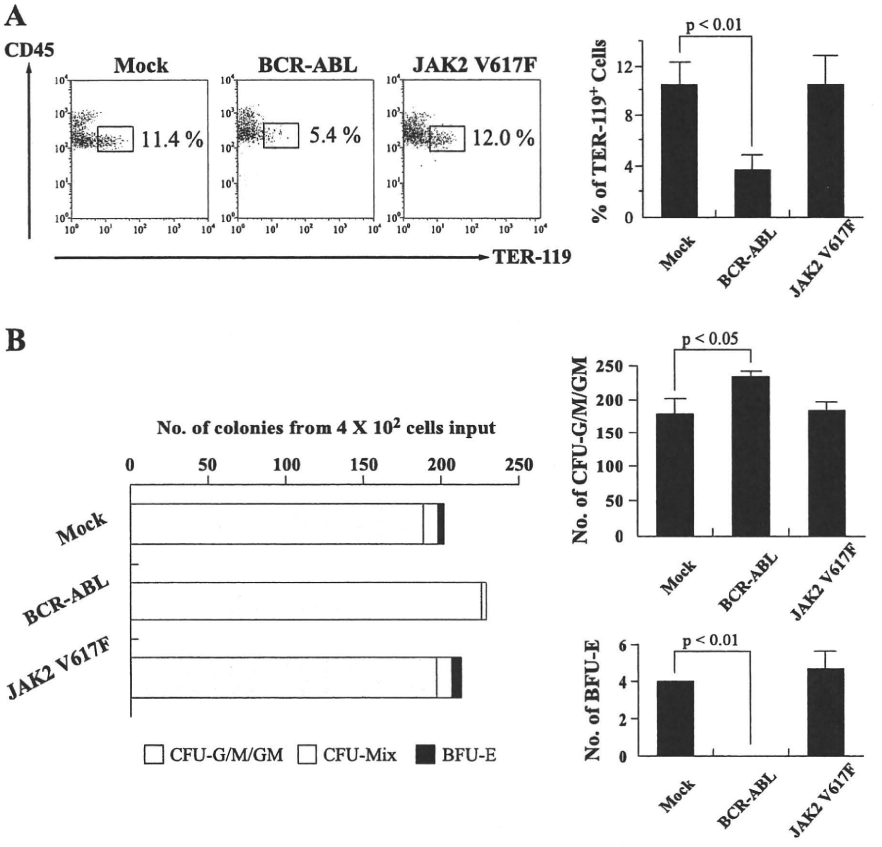

FIGURE 1. **Effects of oncogenic TKs on proliferation of erythroid cells.** *A*, after infection of retrovirus expressing Mock, BCR-ABL, or JAK2 V617F into murine LSK cells, GFP$^+$ cells were sorted and cocultured with MS-5 in the presence of rmSCF and rhEPO. After 5-day cultures, expression of CD45 and TER-119 was analyzed by flow cytometry (*left panels*). The proportions of CD45^{low}TER-119$^+$ cells are shown in the *right bar graph* (n = 3). *B*, respective retrovirus-transduced LSK cells were seeded at a density of 2.0 × 10^2 cells/35-mm dish in methylcellulose medium containing rmSCF, rmIL-3, rmIL-6, rhTPO, and rhEPO. Colony numbers were counted after 9 days. Representative colony numbers (*left*) and myeloid/erythroid colony numbers (*right*, n = 3) are shown. BFU-E, burst-forming units-erythroid; CFU-G/M/GM, colony-forming unit-granulocyte/macrophage/granulocyte-macrophage.

cells treated with manumycin A, a potent farnesyltransferase inhibitor which selectively suppresses Ras, or vehicle only. As shown in Fig. 2*F*, phosphorylation of ERK was reduced by Ras inhibition, indicating that BCR-ABL activates ERK through the activation of Ras. These data indicate that different growth status of erythroid cells between these TKs might result from the preferential activation of Ras signal by BCR-ABL.

Suppression of Ras Signal Ameliorates the Inhibition of Erythropoiesis Caused by BCR-ABL—Furthermore, to make sure that suppressed erythropoiesis caused by BCR-ABL is due to the activation of Ras signal, we examined the effects of Ras-inhibition on erythroid colony formation of BCR-ABL expressing cells. CD34$^+$ cells were separated from BM samples of three patients with newly diagnosed chronic-phase CML. They were then cultured in methylcellulose medium containing rhSCF, rhIL-3, and rhEPO, with or without manumycin A. Complete blockage of Ras signal by supplement of sufficient dose (10 μM) of manumycin A eradicated erythroid colony formation (data not shown). However, as shown in Fig. 2*G*, the number of erythroid colonies was restored by low doses of manumycin A in all three patients, though there was some difference in degree. This result, actually in primary CML cells, supports our model that, although Ras is indispensable for erythroid cell survival, excessive Ras signal downstream of BCR-ABL rather inhibits erythroid cell proliferation.

GATA-1 Inhibits Ras-dependent Cell Proliferation and Survival—As described above, oncogenic Ras signaling promoted the proliferation of myeloid cells, but inhibited that of erythroid cells. To elucidate the mechanisms underlying the different responses to oncogenic Ras between the two lineages, we examined the effects of GATA-1, which is expressed in erythroid cells but not in myeloid cells, on Ras signal. For this purpose, we transduced N-RasE12 and G1ERT, a chimera gene consisting of full-length GATA-1 and the mutated ligand-binding domain of estrogen receptor, into Ba/F3 cells, which was named Ba/F3/N-RasE12/G1ERT. G1ERT reveals GATA-1 activity in response to 4-HT as previously reported (22). As shown in Fig. 3*A*, N-RasE12 enabled this clone to proliferate and survive independently of IL-3. However, when GATA-1 activity was induced by 4-HT treatment, N-RasE12-dependent cell growth was completely suppressed (Fig. 3*A*). In agreement with this result, the proportion of growing cells in S-G2/M phase was reduced by 4-HT treatment from 36% to 8% in DNA contents analysis (Fig. 3*B*). Furthermore, 4-HT treatment induced apoptosis in 78% of cells, which was detected as a subdiploid fraction. From these results, we speculated that GATA-1 might inhibit oncogenic Ras activities, which transmit proliferation and survival signals.

GATA-1 Suppresses MEK Activity—Ras signal is known to be transmitted to the nucleus through Raf, MEK, and ERK in this order. To identify which molecule was inhibited by GATA-1 in this pathway, we performed luciferase assays using a reporter gene for ERK (3 × AP-1-Luc) in NIH3T3 and Ba/F3 cells. As shown in Fig. 4, *A* and *B*, GATA-1 significantly reduced the N-Ras- and MEK1-induced AP-1-luciferase activities almost to the baseline levels (*white boxes*), which indicates that GATA-1 inhibits Ras signal at the level or downstream of MEK. Next, we examined the phosphorylation status of MEK1/2 and ERK1/2 in Ba/F3/N-RasE12/G1ERT cells by immunoblot analysis. As shown in Fig. 4*C*, both MEK1/2 and ERK1/2 were phosphorylated by N-RasE12 even under the culture without IL-3, which was suppressed by 4-HT in a time-dependent manner. This

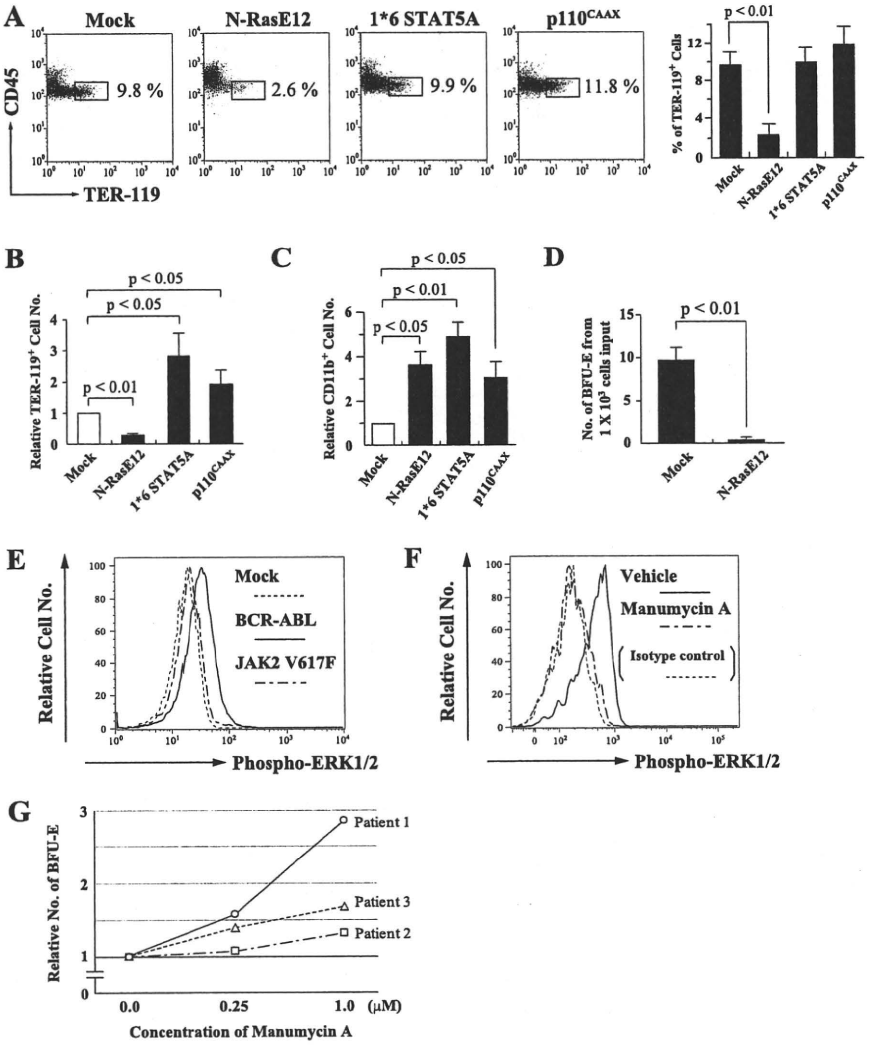

FIGURE 2. **Roles of downstream molecules of oncogenic TKs in erythropoiesis.** *A–C*, LSK cells each transfected with the indicated gene were cocultured with MS-5 in the medium containing rmSCF and rhEPO. After 5 days, expression of CD45 and TER-119 was analyzed by flow cytometry (*A*, *left panels*) and the proportions of CD45^{low}TER-119^{+} cells are shown (*A*, *right bar graph*, $n = 3$). Numbers of the TER-119^{+} cells were calculated by multiplication of the frequencies and total cell numbers. Relative numbers to Mock are shown (*B*). Relative CD11b^{+} myeloid cell numbers are shown (*C*). *D*, retrovirus-infected LSK cells were seeded at a density of 5.0 × 10^2 cells/dish in methylcellulose medium containing rmSCF, rmIL-3, and rhEPO. The numbers of BFU-E were counted after 8 days ($n = 3$). *E*, LSK cells, each transfected with Mock, BCR-ABL, or JAK2 V617F, were further incubated without cytokines after the coculture with MS-5, and the phosphorylation status of ERK1/2 was analyzed using Phosflow technology. *F*, after 5-h incubation of CML patients blood mononuclear cells with manumycin A (7 μM) or vehicle, the phosphorylation status of ERK1/2 was analyzed. *G*, CD34^{+} cells were separated from BM samples of three CML patients, and seeded in methylcellulose medium containing rhSCF, rhIL-3, and rhEPO, with manumycin A at the indicated concentrations or vehicle. The numbers of BFU-E were counted after 9 days, and shown as relative numbers to vehicle in each patient.

result implies that GATA-1 suppresses Ras signal at the level or upstream of MEK. Together with the results from luciferase assays, it was speculated that GATA-1 would inhibit MEK activity.

GATA-1 Blocks the Ras Signal through Its Direct Interaction with MEK1—To clarify how GATA-1 inhibits MEK activities, we examined the interaction between GATA-1 and MEK1. First, we transfected 293T cells with hemagglutinin-tagged (HA-tagged) GATA-1 and/or Flag-tagged MEK1. Total cellular lysates were prepared after 36 h, and GATA-1 was immunoprecipitated with the anti-HA Ab and MEK1 with the anti-Flag Ab. As shown in Fig. 4*D*, immunoblotting with the anti-Flag Ab showed that MEK1 was coimmunoprecipitated with GATA-1 only when both molecules were cotransduced. Also, immunoblotting with the anti-HA Ab showed that GATA-1 was coimmunoprecipitated with MEK1.

Next, to examine whether endogenous GATA-1 and MEK interact in primary erythroid cells, we performed a coimmunoprecipitation analysis using murine BM erythroid cells: Cells positive for CD71 (transferrin receptor), which is expressed at high levels on erythroid progenitors, were purified using the MACS immunomagnetic separation system. Total cellular lysate was prepared and subjected to immunoprecipitation with an anti-GATA-1 Ab or rat isotype IgG. Fig. 4*E* shows that MEK is coimmunoprecipitated with GATA-1, indicating that these molecules actually interact with each other in primary erythroid cells.

Finally, we investigated whether MEK1 directly binds to GATA-1 *in vitro* by GST pull-down assays. After verifying the quality and quantity of GST-MEK1 fusion protein by Coomassie Brilliant Blue staining (data not shown), we analyzed the binding between GST-MEK1 and *in vitro*-translated GATA-1. As shown in Fig. 4*F*, GST-MEK1 but not GST alone, bound to ^{35}S-labeled GATA-1 *in vitro*.

Together with the results of Fig. 4, *A–C*, we proved the following two facts: GATA-1 inhibits MEK activation; GATA-1 and MEK interact with each other in primary erythroid progenitors. From these facts, we speculated that GATA-1 blocks Ras signal at least partly through the direct interaction with MEK1.

Oncogenic Ras Induces Suppression of Erythropoiesis through the Induction of p21$^{CIP1/WAF1}$—In addition to the functions to deliver mitogenic and anti-apoptotic signals (14), Ras paradoxically causes growth arrest (senescence) in normal cells through several cell cycle regulatory molecules such as p53, p16^{INK4a}, p19^{ARF}, and p21$^{CIP1/WAF1}$ (15, 21). Among them, p53 is a tumor-suppressor and acts as a pivotal regulator of these responses (15, 16, 19, 21). p19^{ARF} is a splicing variant of p16^{INK4a} and inhibits the function of H/MDM2, which pro-

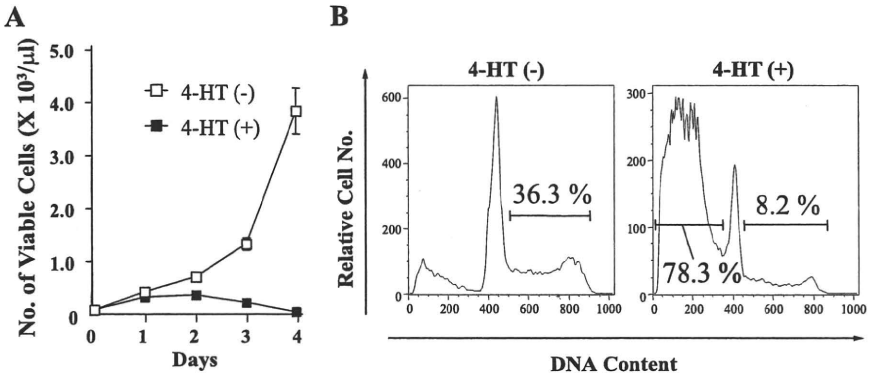

FIGURE 3. **Inhibition of Ras-dependent cell proliferation and survival by GATA-1.** *A*, Ba/F3/N-RasE12/G1ERT cells were seeded at a density of 100/μl and cultured in RPMI supplemented with 1% FBS without IL-3 in the presence or absence of 1 μM 4-HT. Total numbers of viable cells were counted by trypan blue dye exclusion method on the indicated days. The results are shown as means ± S.D. of triplicate cultures. *B*, after 48 h of culture, DNA contents of 4-HT-treated or untreated cells were examined by propidium iodide staining. The proportions of cells in S-G2/M phase and subdiploid fraction are shown, respectively.

motes degradation of p53 (30). p16^{INK4a} is a member of the INK4 family of CDK inhibitors, which causes cell cycle arrest at G1 phase by inhibiting CDK4/6 activities (30). Meanwhile, p21$^{CIP1/WAF1}$ is a member of the Cip/Kip family of CDK inhibitors and also induces G1 arrest by inhibiting CDK2 activities. In this report, we next examined their roles in N-RasE12-induced suppression of erythropoiesis.

At first, we examined the effects of N-RasE12 on the expression of p16^{INK4a}, p19^{ARF}, and p21$^{CIP1/WAF1}$ by semiquantitative/real-time RT-PCR analyses or immunofluorescence. As shown in Fig. 5*A* and *B*, the expression of p16^{INK4a} and p19^{ARF} was induced in N-RasE12-transduced LSK cells both in mRNA and protein levels. Also, the expression of p21$^{CIP1/WAF1}$ was increased by nearly 2-fold in N-RasE12-transduced LSK cells compared with mock-transduced LSK cells (Fig. 5*C*), suggesting that the up-regulated p16^{INK4a}, p19^{ARF}, and/or p21$^{CIP1/WAF1}$ might be involved in N-RasE12-induced suppression of erythropoiesis.

To further analyze the roles of these molecules, we next introduced N-RasE12 into LSK cells isolated from p16^{INK4a}/p19^{ARF} double knock-out (KO) mice, cocultured them with MS-5, and examined the development of erythroid cells by flow cytometry. As shown in Fig. 6*A*, the frequency of CD45^{low}TER-119^{+} erythroid cells was a little lower in N-RasE12-transduced double KO cells than in N-RasE12-transduced WT cells (WT 1.8% *versus* double KO 0.8%) (*upper panels*). In addition, although the number of these erythroid cells was slightly restored in N-RasE12-transduced double KO cells compared with N-RasE12-transduced WT cells (*lower graph*), this difference was not significant.

We also introduced N-RasE12 into LSK cells isolated from p21$^{CIP1/WAF1}$-null mice. As observed in the other experiments, N-RasE12 reduced the proportion of CD45^{low}TER-119^{+} erythroid cells both in WT and p21$^{CIP1/WAF1}$-null LSK cells (Fig. 6*B*, *upper panels*). However, p21$^{CIP1/WAF1}$ deficiency partially, but significantly, restored the proportion of this fraction from 3.0 to 5.2%. In addition, surprisingly, N-RasE12 increased the number of erythroid cells in p21$^{CIP1/WAF1}$-null LSK cells compared with mock-transduced LSK cells (Fig. 6*C*, *lower graph*), indicating that p21$^{CIP1/WAF1}$ is a major regulator of N-RasE12-induced suppression of erythropoiesis.

Because the expression of p21$^{CIP1/WAF1}$ is regulated in p53-dependent and independent manners (31–33), we finally investigated the roles of p53 in N-RasE12-induced suppression of erythropoiesis with the similar experiment. As shown in Fig. 6*C*, the proportion and number of erythroid cells in mock-transduced LSK cells were reduced by p53 deficiency. In addition, p53 deficiency did not cancel the inhibition of erythroid cell development by N-RasE12. Together, these results indicate that N-RasE12 inhibits erythropoiesis through p21$^{CIP1/WAF1}$ in a p53-independent manner.

DISCUSSION

We here found that BCR-ABL suppresses erythroid cell proliferation. This finding is largely consistent with clinical features of CML, in which anemia is commonly observed and erythroid blast crisis is a rare event. Also, we found that constitutively activated Ras, but not PI3-K or STAT5, inhibits erythropoiesis and that a farnesyltransferase inhibitor, manumycin A, restores erythroid colony formation of CML patients BM cells at relatively low concentrations. These results strongly indicate that Ras is a negative regulator of erythropoiesis downstream of BCR-ABL. So far, functions of Ras in normal erythropoiesis are controversial. It was reported that Ras signaling was essential for development of erythroid progenitors (34, 35). In contrast, H-Ras$^{-/-}$, N-Ras$^{-/-}$, and double KO (H-Ras$^{-/-}$ N-Ras$^{-/-}$) mice had no apparent hematopoietic abnormality, indicating that Ras is dispensable for normal erythropoiesis (36, 37). Regarding the roles of oncogenic Ras in erythropoiesis, it was shown that oncogenic H-Ras blocks terminal erythroid differentiation (38), and that enforced expression of an active mutant of N-Ras in primitive hematopoietic cells inhibits proliferation of erythroid cells (17, 18). Our results indicate that the excessive Ras signal would inhibit erythropoiesis, though Ras signal might be to some extent necessary for erythroid cell survival. Ras is mutated in a significant proportion of cases with acute myeloid leukemia and myelodysplastic syndromes (39), or constitutively activated by various oncogenic TKs, including FLT3-ITD (2), c-KIT D816V (40), and TEL-PDGFRB (41). So, anemia observed in these hematologic malignancies also might be, at least partly, attributed to the constitutively activated Ras signal. However, in this study, JAK2 V617F slightly enhanced erythropoiesis as observed in patients with PV, whereas its downstream pathways including Ras, PI3-K, and STAT5 are common to BCR-ABL (1, 5). As for this difference, we here found that JAK2 V617F does not activate Ras signal so strongly as BCR-ABL. Also, it was speculated that JAK2 V617F would utilize mainly STAT5 to promote erythropoiesis in PV patients. Although Ras has some isoforms, we focused on N-Ras,